Received: 7 December 2020 | Revised: 29 January 2021 | Accepted: 3 February 2021

DOI: 10.1111/apha.13623

REGULAR PAPER

ACTA PHYSIOLOGICA

Insulin differentially modulates GABA signalling in hippocampal neurons and, in an age-dependent manner, normalizes GABA-activated currents in the tg-APPSwe mouse model of Alzheimer's disease

Hayma Hammoud[1]* | **Olga Netsyk[1]*** | **Atieh S. Tafreshiha[1]** | **Sergiy V. Korol[1]†** | **Zhe Jin[1]†** | **Jin-Ping Li[2]** | **Bryndis Birnir[1]**

[1]Department of Medical Cell Biology, Uppsala University, Uppsala, Sweden

[2]Department of Medical Biochemistry and Microbiology, Uppsala University, Uppsala, Sweden

Correspondence
Bryndis Birnir, Department of Medical Cell Biology, Uppsala University, Uppsala, Sweden.
Email: bryndis.birnir@mcb.uu.se

Funding information
The study was funded mainly by the Swedish Research Council grants 2018-02952 and 2015-02417 to BB but also by grants from Excellence of Diabetes Research in Sweden (EXODIAB) to BB and SVK, the Swedish Brain Foundation to BB and, in part, by a Swedish Research Council grant 2018-02503 to JPL.

Abstract

Aim: We examined if tonic γ-aminobutyric acid (GABA)-activated currents in primary hippocampal neurons were modulated by insulin in wild-type and tg-APPSwe mice, an Alzheimer's disease (AD) model.

Methods: GABA-activated currents were recorded in dentate gyrus (DG) granule cells and CA3 pyramidal neurons in hippocampal brain slices, from 8 to 10 weeks old (young) wild-type mice and in dorsal DG granule cells in adult, 5-6 and 10-12 (aged) months old wild-type and tg-APPSwe mice, in the absence or presence of insulin, by whole-cell patch-clamp electrophysiology.

Results: In young mice, insulin (1 nmol/L) enhanced the total spontaneous inhibitory postsynaptic current ($sIPSC_T$) density in both dorsal and ventral DG granule cells. The extrasynaptic current density was only increased by insulin in dorsal CA3 pyramidal neurons. In absence of action potentials, insulin enhanced DG granule cells and dorsal CA3 pyramidal neurons miniature IPSC (mIPSC) frequency, consistent with insulin regulation of presynaptic GABA release. $sIPSC_T$ densities in DG granule cells were similar in wild-type and tg-APPSwe mice at 5-6 months but significantly decreased in aged tg-APPSwe mice where insulin normalized currents to wild-type levels. The extrasynaptic current density was increased in tg-APPSwe mice relative to wild-type littermates but, only in aged tg-APPSwe mice did insulin decrease and normalize the current.

Conclusion: Insulin effects on GABA signalling in hippocampal neurons are selective while multifaceted and context-based. Not only is the response to insulin related to cell-type, hippocampal axis-location, age of animals and disease but also to the subtype of neuronal inhibition involved, synaptic or extrasynaptic $GABA_A$ receptors-activated currents.

*Hayma Hammoud and Olga Netsyk are co-first authors and contributed equally.

†Sergiy V. Korol and Zhe Jin contributed equally.

KEYWORDS

CA3 pyramidal neuron, dentate gyrus granule cell, $GABA_A$ receptor, hippocampus, IPSC, tonic current

1 | INTRODUCTION

Insulin is secreted by the pancreatic islet beta cells and regulates glucose homeostasis in the periphery.[1] For a long time, the brain was thought to be insulin insensitive, as glucose utilization in the central nervous system (CNS) does not rely on insulin.[2,3] In recent years, evidence has emerged indicating that insulin facilitates critical brain functions including learning, cognition and motivated behaviour, implying that insulin signalling is an important part of the healthy brain.[2-4] Insulin receptors (IR) are prominently expressed in many areas of the brain, including the cortex and the hippocampus.[5,6] Insulin enters the brain, by crossing the blood-brain barrier by a saturable transport system[3,7,8] and insulin can even be made in subsets of neuroglial cells.[9,10] How insulin modulation of neuronal plasticity comes about and what the effects are on neuronal function is still being explored.

It is well-documented that the effectiveness of the metabolic hormonal systems declines with age and the deficiency of function that may result in associated with faster ageing and an increased risk of developing neurodegenerative diseases.[11-14] Insulin sensitivity decreases with ageing[13,15] and epidemiological data suggest that the diminished insulin signalling may increase the propensity for development of cognitive dysfunction and progression of AD in humans and rodents.[11,12,16] Insulin has further been indicated having a protective role in relation to the progressive pathogenesis of AD[2,17] amyloid plaques and neurofibrillary tangles may be decreased by insulin.[18] In some patients with AD, intranasal insulin improved memory function.[19] AD is characterized by loss of synapse density and degeneration of at least cholinergic and glutamatergic pathways in the brain.[20] Although it is generally accepted that there is a widespread disruption of the excitatory pathways in the brain, it has been assumed that the inhibitory GABAergic pathways are preserved.[21,22] However, evidence from functional studies on $GABA_A$ receptors from human AD brains have shown that this is not the case. Indeed, a large reduction and remodelling of GABA signalling is observed in AD and it may explain, at least in part, the cortical disinhibition in several areas of the AD brain, resulting in hyperexcitability and is correlated with the level of dementia.[23,24] These results are, perhaps, not so surprising considering that GABA is the main inhibitory neurotransmitter in the central nervous system and regulates the excitability of all neurons in mammalian brains.

GABA binds to $GABA_A$ and $GABA_B$ receptors in neurons. The $GABA_A$ receptors are chloride ion channels opened by GABA and are located at inhibitory synapses and also outside of synapses where they are termed extrasynaptic $GABA_A$ receptors. The receptors mediate functionally distinct types of inhibition: the fast point-to-point synaptic transmission is mediated by high concentrations (millimolar) of GABA, activating synaptic $GABA_A$ receptors, whereas the extrasynaptic $GABA_A$ receptors are activated by low micro to sub-micromolar GABA concentrations or spontaneously opening channels, and mediate a persistent form of inhibition. The GABA-activated inhibitory currents in a neuron then result from the summation of inhibitory postsynaptic currents[25-29] and from extrasynaptic $GABA_A$ receptors currents.[29-36] Synaptic currents activated by spontaneous firing of interneurons are termed sIPSCs and the action-potential independent currents, mIPSCs.[25-29]

It is well-recognized that hippocampal hyperactivity is one of the earliest dysfunctions and a feature of AD in humans and numerous transgenic AD mice.[37,38] The DG of the dorsal hippocampus plays an important role in memory formation and is among the first regions where plaques are deposited in AD. In DG granule cells, increased extrasynaptic $GABA_A$ receptor-mediated current impaired long-term potentiation and memory formation in mouse models of AD[39-41] and insulin treatment decreased intracellular amyloid-β (Aβ) whereas insulin/insulin receptor dysfunction increased Aβ accumulation in AD model mice.[2,42] Moreover, it has been known since the early 1980s that insulin can inhibit spontaneous firing in rat hippocampal pyramidal neurons.[43] Nevertheless, to-date the knowledge of effects of insulin on GABA signalling in the hippocampal sub-regions is limited.[3,43,44]

Electrophysiological properties of hippocampal neurons along the hippocampal longitudinal axis vary[29,45-50] and there appears to be increasing neuronal excitability from the dorsal to the ventral pole of the hippocampus.[47,49,51-54] A number of different mechanisms have been proposed to explain the observed higher excitability of the ventral hippocampus, including reduced inhibitory GABAergic tone.[53] We recently showed, in eight to ten weeks old wild-type mice, that characteristic tonic GABA-activated currents are recorded in hippocampal primary neurons according to the cell-type and the dorsoventral hippocampal-axis location.[29] Here, we examined if insulin modulates tonic GABA-activated conductance in DG granule cells and CA3 pyramidal neurons in dorsal and ventral hippocampus of young, eight to ten weeks old wild-type mice and then, in DG granule cells, if the insulin modulation was intact in older wild-type and tg-APPSwe mice, before and during amyloid plaques formation.

Our results demonstrate that insulin regulates the tonic GABA-activated current density in hippocampal primary neurons according to cell-type, location along hippocampal dorsoventral axis and age. Furthermore, in the diseased aged tg-APPSwe mouse brain, insulin-mediated synaptic plasticity is reevoked and results in normalization to wild-type levels of the fast inhibitory synaptic and extrasynaptic currents densities.

2 | RESULTS

The results section is divided according to the age of the mice: First, insulin effects on GABA-activated currents in DG granule cells and CA3 pyramidal neurons in young, eight to ten weeks old wild-type mice and second, insulin effects on GABA-activated currents in dorsal DG granule cells in adult, 5-12 months old wild-type and tg-APPSwe mice.

2.1 | Young mice

2.1.1 | Insulin receptor expression in the mouse dorsal and ventral hippocampus

Insulin binds to the IR and activates downstream cellular signalling pathways. We examined the expression of the IR in the mouse dorsal and ventral hippocampus by incubating hippocampal sections with an insulin receptor-specific antibody. IR labelling in Figure 1 is indicated by the dark brown colour. The CA1-CA3 pyramidal neuronal and the DG granule cells layers were robustly labelled in both the dorsal and the ventral hippocampus. The specificity of the IR antibody was validated as shown in Figure S1.

2.1.2 | Insulin differentially modulated IPSCs and the extrasynaptic current in DG granule cells and CA3 pyramidal hippocampal neurons

The dorsal and ventral primary hippocampal neurons are engaged in neuronal networks that have different physiological functions.[53,55] It is possible that hormones like insulin that enter the brain, differentially regulate the networks along the hippocampal dorsoventral axis. To gain insight into the insulin regulation of the circuitry, we examined the normal functional characteristic of the sIPSCs, mIPSCs and extrasynaptic currents in DG granule cells and CA3 pyramidal neurons in the dorsal and ventral mouse hippocampus and then, how the currents were modulated by insulin. In order to selectively activate the IR, we applied insulin at near-physiological concentration (1 nmol/L) to exert its physiological effect.[44,56] Higher insulin concentrations can cause non-specific effect via activation of insulin-like growth factors receptors.

DG granule cells

Characteristic currents and the effects of insulin on sIPSCs are shown in Figure 2, at a slow (min) and a fast (s) time-scale, for the dorsal (Figure 2Aa,b) and the ventral (Figure 2Ba,b)

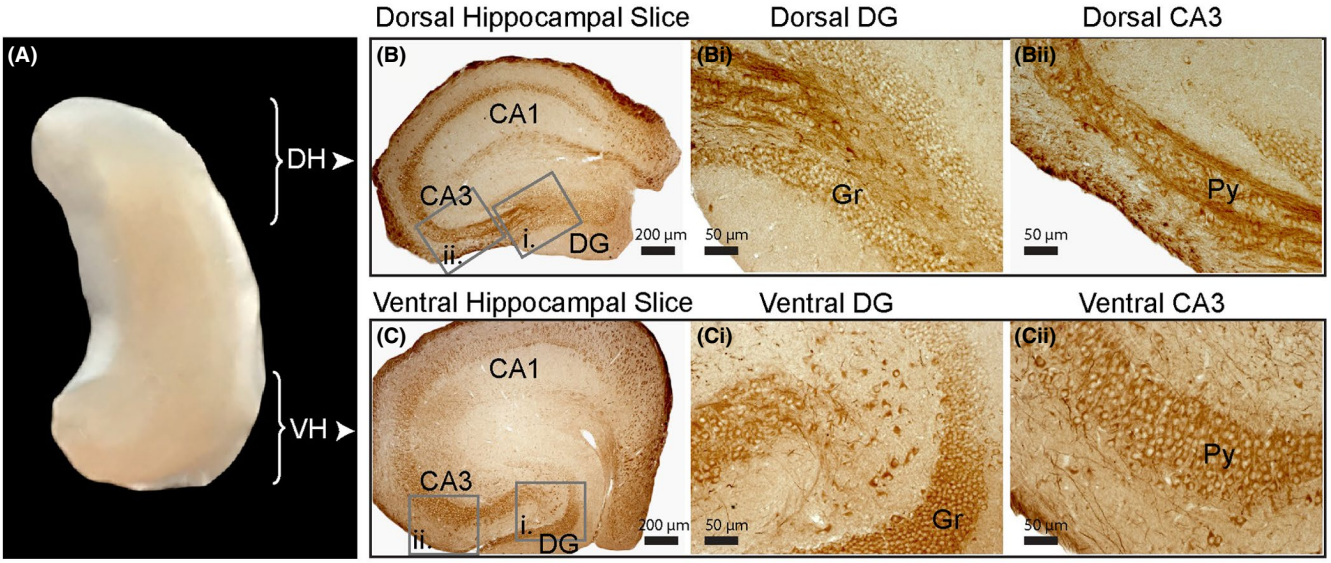

FIGURE 1 Immunostaining of the insulin receptor along the dorsoventral axis of the mouse hippocampus. (A), A microphotograph of the isolated mouse hippocampus (approx. 6 mm length): dorsal (DH) and ventral (VH) hippocampal regions. Immunohistochemical staining of the mouse hippocampus labelled with insulin receptor (IR, brown colour) antibody in CA1, CA3 and dentate gyrus (DG) of DH (B) and VH (C). DG granule cells display a staining signal of IR in the DH and VH (Bi and Ci). In the CA3 regions, the layer of pyramidal neurons cell bodies shows IR expression (Bii and Cii). The experiment was repeated in four animals and the same pattern of staining was observed in all of them. Gr: stratum granulosum; Py: stratum pyramidale

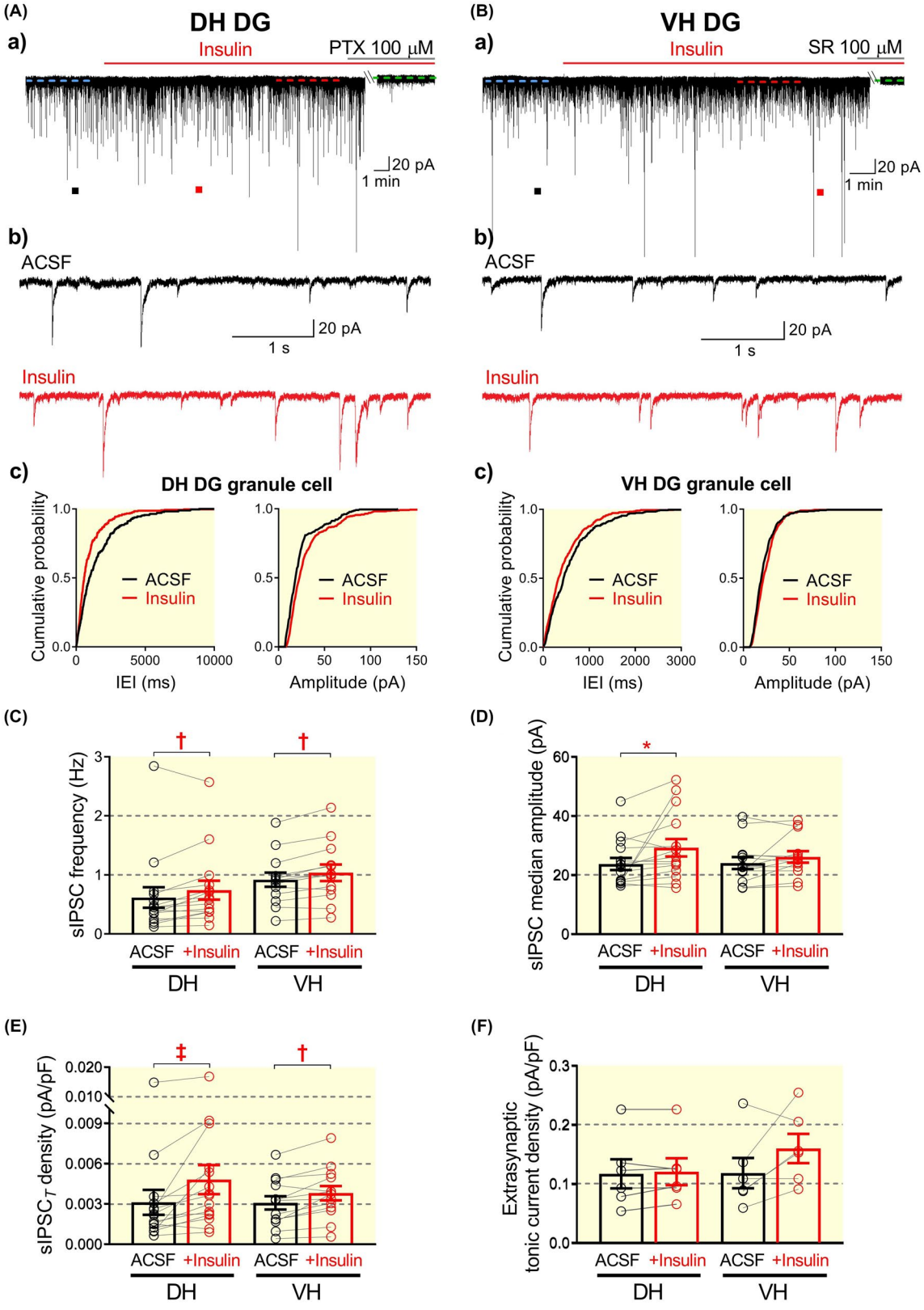

DG granule cells. Insulin (1 nmol/L) increased the mean sIPSC frequency by about 21% and 13% in the dorsal and ventral hippocampal DG granule cells, respectively (Figure 2Ac, Bc,C), whereas the median amplitude of sIPSCs was only increased (~ 23%) in the dorsal hippocampus (Figure 2D). The sIPCSs rise-time was faster in the ventral hippocampus in the presence of insulin but no effect was recorded on the current decay (Figure S2A). As

FIGURE 2 Insulin potentiated synaptic but not extrasynaptic $GABA_A$ receptor-mediated currents in the dentate gyrus granule cells in dorsal and ventral mouse hippocampus. A and B, Representative traces of GABAergic currents recorded from DG granule cells in dorsal (DH, Aa) and ventral (VH, Ba) hippocampus under bath insulin (1 nmol/L) application. The difference between the dashed lines indicates the tonic current amplitude. Marked regions with filled squares (*top*, a) are shown on an expanded scale below (b, 5 s long segments) the whole trace: sIPSCs recorded under control conditions (*black colour*) and insulin application (*red trace*) from DH (Ab) and VH (Bb) correspondingly. Examples of cumulative probability plots for the inter-event interval (IEI) and median amplitude of sIPSCs calculated from DG granule cell of the DH (Ac; from representative trace Aa) and the VH (Bc; from representative trace Ba) under control conditions (ACSF, *black line*) and under insulin application (*red line*). The left shift of the cumulative probability curve after bath perfusion of 1 nmol/L insulin (*red line*) indicates a decrease of sIPSCs IEI (that corresponds to increased sIPSCs frequency) in DG granule cell of DH (Ac *left*; IEI; 273 vs 303 events analysed for ACSF vs insulin correspondingly) and VH (Bc *left*; IEI; 303 events analysed for ACSF and 516 events – for insulin application). The right shift of the cumulative distribution curve after application of 1 nmol/L insulin (*red line*) represents an increase of sIPSCs median amplitude in DG granule cell of DH (Ac *right*, Amplitude; 230 vs 392 events analysed for ACSF vs insulin correspondingly). To plot cumulative distribution curve for IPSCs amplitude from ventral DG granule cell (Bc *right,* Amplitude) 297 events were analysed for ACSF (*black line*) and 436 events for insulin (*red line*) conditions. Summary statistics of frequency (C), median amplitude (D) and total current density ($sIPSC_T$ density, E) of sIPSC recorded from DG granule cells of DH (n = 15 cells) and VH (n = 13 cells) under control (*ACSF, black colour*) and 1 nmol/L insulin application (*red colour*). Extrasynaptic current density (F) in dentate granule cells of DH (n = 6 cells) and VH (n = 6 cells) recorded under control conditions (*ACSF, black colour*) and after insulin perfusion (*red colour*). Data are presented as scatted dot plot for individual values and as bar plot for mean ± SEM. Connected lines indicate data obtained from individual cells before (*black*) and during insulin application (*red*). Only statistically significant differences are marked on the graph. The Wilcoxon matched-pairs signed rank test, $^{*}P < .05$, $^{\dagger}P < .01$, $^{\ddagger}P < .001$. $V_{hold} = -60$ mV

the DG granule cells at the two hippocampal poles vary in size,[29] we calculated the sIPSC density. Insulin increased the mean sIPSC density by ~54% and ~22% in the dorsal and ventral DG granule cells, respectively (Figure 2E). In contrast, insulin had no effect on the mean extrasynaptic current density in the dorsal or the ventral hippocampal DG granule cells (Figure 2F).

The potentiation of the sIPSCs by insulin can be related to pre- or postsynaptic mechanisms. We, therefore, examined the effects of insulin (1 nmol/L) on mIPSCs in the presence of TTX (1 μmol/L) which blocks voltage-gated sodium channels and thus, action potential-dependent GABA release. Representative current traces are shown in Figure 3, at a slow (min) and a fast (s) time-scale, for the dorsal (Figure 3Aa,b) and the ventral (Figure 3Ba,b) DG granule cells. Insulin increased the mean mIPSC frequency in the granule cells by ~21% in the dorsal and ~15% in the ventral hippocampus (Figure 3Ac, Bc,C), similar to what was observed for the sIPSCs, consistent with increased probability of GABA release from the presynaptic terminals in the presence of insulin. The median amplitude of the mIPSCs was not altered by insulin (Figure 3D) but the median decay time was prolonged in the dorsal DG granule cells (Figure S2Bb). Only in the ventral DG granule cells did insulin significantly increase the mIPSC density (~23%). No effect of insulin was recorded on the extrasynaptic current density (Figure 3F).

CA3 pyramidal neurons

Characteristic currents and the effects of insulin on sIPSCs are shown in Figure 4, at a slow (min) and a fast (s) time-scale, for the dorsal (Figure 4Aa,b) and the ventral (Figure 4Ba,b) CA3 pyramidal neurons. Insulin did not modify the sIPSC frequency, median amplitude or kinetics in the dorsal or ventral CA3 pyramidal neurons (Figure 4A-E; Figure S3A). In contrast, insulin almost doubled the mean extrasynaptic current density in the dorsal CA3 pyramidal neurons (Figure 4F).

The potentiation of the extrasynaptic current by insulin can be related to either pre- or postsynaptic mechanisms. We, therefore, examined the effects of insulin (1 nmol/L) on the mIPSCs in the presence of TTX (1 μmol/L). Representative current traces are shown in Figure 5, at a slow (min) and a fast (s) time-scale, for the dorsal (Figure 5Aa,b) and the ventral (Figure 5Ba,b) CA3 pyramidal neurons in the presence of TTX, without or with insulin (1 nmol/L). The mean frequency of mIPSCs was significantly increased by insulin but only in the dorsal CA3 pyramidal neurons (~18%) (Figure 5C) and, is consistent with increased presynaptic GABA release probability. The median amplitude of the currents and kinetic parameters under insulin application were similar to the control currents for both the dorsal and ventral CA3 pyramidal neurons (Figure 5Ac, Bc,D; Figure S3B). In the dorsal CA3 pyramidal neurons, insulin increased the mIPSC density (~26%, Figure 5E) but no longer enhanced the extrasynaptic current density when TTX blocked the action potentials. The results are consistent with decreased spill-over of GABA when action potential-dependent GABA release ceased.

Extrasynaptic $GABA_A$ receptors containing α5 subunit are expressed in CA3 pyramidal cells.[57] We examined if the insulin-enhanced tonic current was mediated by these receptors (Figure S4). Bath application of the inhibitors L-655,708 or TB21007, selective for the α5-subtype, did not decrease the tonic current density in dorsal CA3 neurons neither in control (0.007 ± 0.004 pA/pF, n = 5) nor when insulin was

applied (0.006 ± 0.004 pA/pF, n = 7; Figure S4). In order to examine if lower affinity receptors could be activated and modulated by insulin, we applied 5 μmol/L GABA but the results were similar and not significantly different (control: 0.062 ± 0.014 pA/pF (n = 5); in insulin: 0.105 ± 0.023 pA/pF (n = 8), $P = .1709$, Figure S4).

2.1.3 | PI3-kinase, but not MAPK-kinase (MAPKK), is required for insulin enhancement of the GABA-activated currents

Insulin binding to the IR leads to rapid autophosphorylation of the receptor, followed by phosphorylation of the

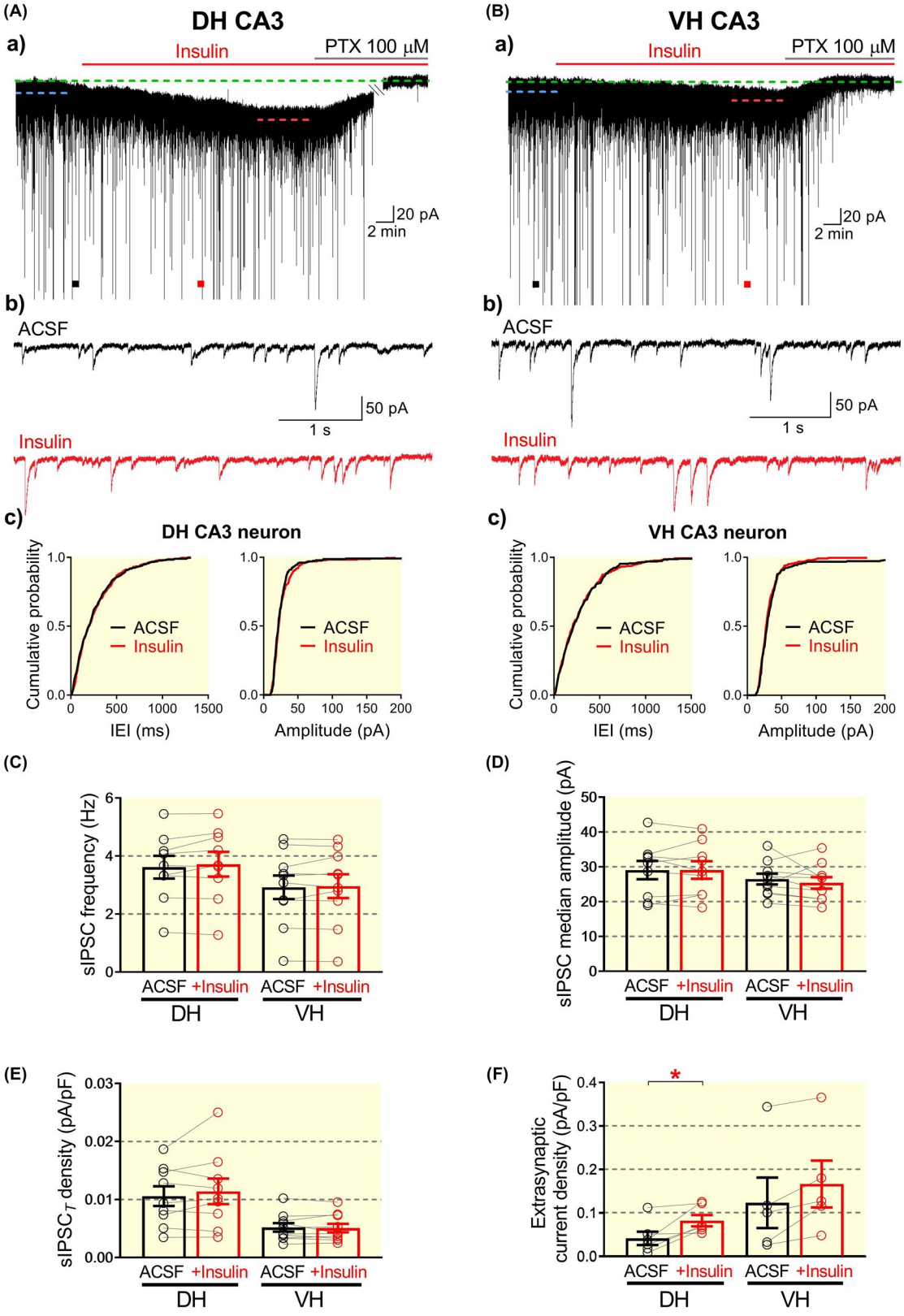

FIGURE 3 Insulin increased the mIPSCs frequency and the $mIPSC_T$ density in the dentate gyrus granule cells of the mouse hippocampus. Representative inhibitory current traces from DG granule cells of dorsal (DH, A) and ventral (VH, B) hippocampus in the presence of TTX (1 μmol/L) under insulin (1 nmol/L) application. Marked regions with filled squares (*top*, a) are shown on an expanded scale below the whole trace, respectively (b). Short segments represent miniature inhibitory synaptic currents (mIPSCs) recorded from DG granule cells of DH (Ab) and VH (Bb) correspondingly before (*TTX, gray trace*) and during 1 nmol/L insulin application (*dark red trace*) in the constant presence of 1 μmol/L TTX. Cumulative probability plots for the inter-event interval (IEI) and median amplitude of mIPSCs recorded from DG granule cell of the DH (Ac; from representative trace Aa) and the VH (Bc; from representative trace Ba) under control conditions (TTX, *gray line*) and during insulin treatment (TTX + insulin, *dark red line*). The left shift of the cumulative probability curve after bath application of 1 nmol/L insulin (TTX + insulin, *dark red line*) indicates a decrease of mIPSCs IEI (that corresponds to increased frequency of mIPSCs) in DG granule cell of DH (Ac *left*; IEI; 128 vs 207 events analysed for TTX vs TTX + insulin correspondingly) and VH (Bc *left*; IEI; 221 events analysed for TTX and 302 events – for insulin application). The cumulative distribution curves before (*gray line*) and after application of 1 nmol/L insulin (*dark red line*) represent no significant changes of mIPSCs median amplitude in DG granule cell either of DH (Ac *right*; Amplitude; 127 vs 162 events analysed for TTX vs TTX + insulin correspondingly) or VH (Bc *right*, Amplitude; 161 events were analysed for TTX (*gray line*) and 239 events for insulin (TTX + insulin, *dark red line*) conditions). Compiled data showing the frequency (C), median amplitude (D) and total current density ($mIPSC_T$ density, E) of mIPSCs recorded from DG granule cells of DH (n = 8 cells) and VH (n = 7 cells) under control (*TTX, gray colour*) and insulin treatment (*dark red colour*). Summary for extrasynaptic current density (F) in DG granule cells of DH (8 - 10 cells) and VH (6 - 8 cells) recorded in the presence of TTX under control conditions (*TTX, gray colour*) and after 1 nmol/L insulin application (*dark red colour*). Data are presented as dot plot with bar for mean ± SEM. Connected lines indicate data obtained from individual cells before (*gray colour*) and during perfusion with insulin (1 nmol/L, *dark red colour*). Outlier (for non paired data) is detected by the Tukey method and marked as dot plot (*filled circle*). Only statistically significant difference is marked on the graph. The Wilcoxon matched-pairs signed rank test/non-parametric Mann-Whitney *U* test, $*P < .05$. $V_{hold} = -60$ mV

receptors' substrate proteins resulting in activation of downstream signalling pathways including the PI3K and MAPKK cascades.[58] The following sets of experiments aimed to identify the specific insulin-activated intracellular signalling pathway involved in the modulation of the sIPSCs in the DG granule cells and the extrasynaptic current in the dorsal CA3 pyramidal neurons. Hippocampal slices were preincubated with an inhibitor with the aim of blocking a specific intracellular signalling pathway. The PI3-kinase inhibitor wortmannin (100 nmol/L), was applied to block PI3K-mediated signalling and the results are shown in Figure 6A. In DG granule cells in the presence of wortmannin, insulin no longer enhanced the sIPSC frequency (Figure 6Aa,Ba), the median amplitude (Figure 6Aa,Bb) or the total current density (Figure 6Aa,Bc), neither in the dorsal nor the ventral hippocampal slices. Thus, blocking the PI3K signalling completely abolished the insulin-induced potentiation of the sIPSCs in the DG granule cells. In contrast, incubation with the MAPKK inhibitors, U0126 (2 μmol/L) or PD98059 (20 μmol/L), did not alter the insulin effect on the DG granule cells and the results were similar to what was observed with insulin alone (Figure 6Ab,Ca,b,c). For the CA3 pyramidal neurons, in the dorsal hippocampus, incubation with wortmannin (100 nmol/L) abolished the insulin-induced potentiation of the extrasynaptic current density (Figure 6Da,c) whereas the MAPKK inhibitors, U0126 (2 μmol/L) or PD98059 (20 μmol/L), did not alter the insulin effect (Figure 6Db,c). The inhibitors did not modulate the sIPSCs (Figure S5). Together, the results identify regulation of the presynaptic GABA release and the postsynaptic GABA-activated currents by insulin-driven PI3K signalling in the DG granule cells and the CA3 pyramidal neurons.

2.2 | Adult mice

Since insulin modulated GABA-activated currents in the young, eight to ten weeks old mice, we wondered if the modulation was maintained in older animals and in disease. We, therefore, proceeded and recorded GABA-activated synaptic and extrasynaptic currents from DG granule cells in dorsal hippocampal slices from 5 to 12 months old wild-type mice and their tg-APPSwe littermates. This transgenic AD model was selected as the mice exhibit some clinical features characteristic of AD including extracellular Aβ plaque deposition, microgliosis and astrogliosis in the hippocampus at approximately 12 months of age.[59] Intraneuronal Aβ aggregates occur at approximately six months.[60] As age is a risk factor for insulin resistance and AD,[13,61] the age-matched wild-type littermates were used to reveal age-related effects, on the GABA-activated currents during normal ageing.

2.2.1 | Insulin only enhances fast synaptic $GABA_A$ receptor-mediated currents in aged tg-APPSwe mice

Synaptic GABA-activated currents were recorded, before amyloid plaque deposition, in 5-6 months old tg-APPSwe mice (Figure 7A,B; Figure S6), and at the stage of extracellular plaque deposition in 10-12 months old tg-APPSwe mice (Figure 8A,B; Figure S6) and their wild-type littermates. A mutant form of APP (isoform 695) with the Swedish mutation results in elevated levels of Aβ and extracellular amyloid plaque deposition in the hippocampus of tg-APPSwe mice at approximately 10-12 months of age. The plaques were

concentrated in the stratum lacunosum moleculare and the DG (Figure 8A). After electrophysiological recordings, the hippocampal slices were stained with Thioflavin S and extracellular plaques (*bright green*) deposition visualized in the aged tg-APPSwe mice (Figure 8A).

Characteristic current traces and effects of insulin on sIPSCs in DG granule cells in hippocampal slices from 5 to 6 and aged (10-12 months old) mice are shown in Figures 7B and 8B, respectively. In the 5-6 months old animals, the sIPSCs frequency, amplitude, charge transfer and total current were

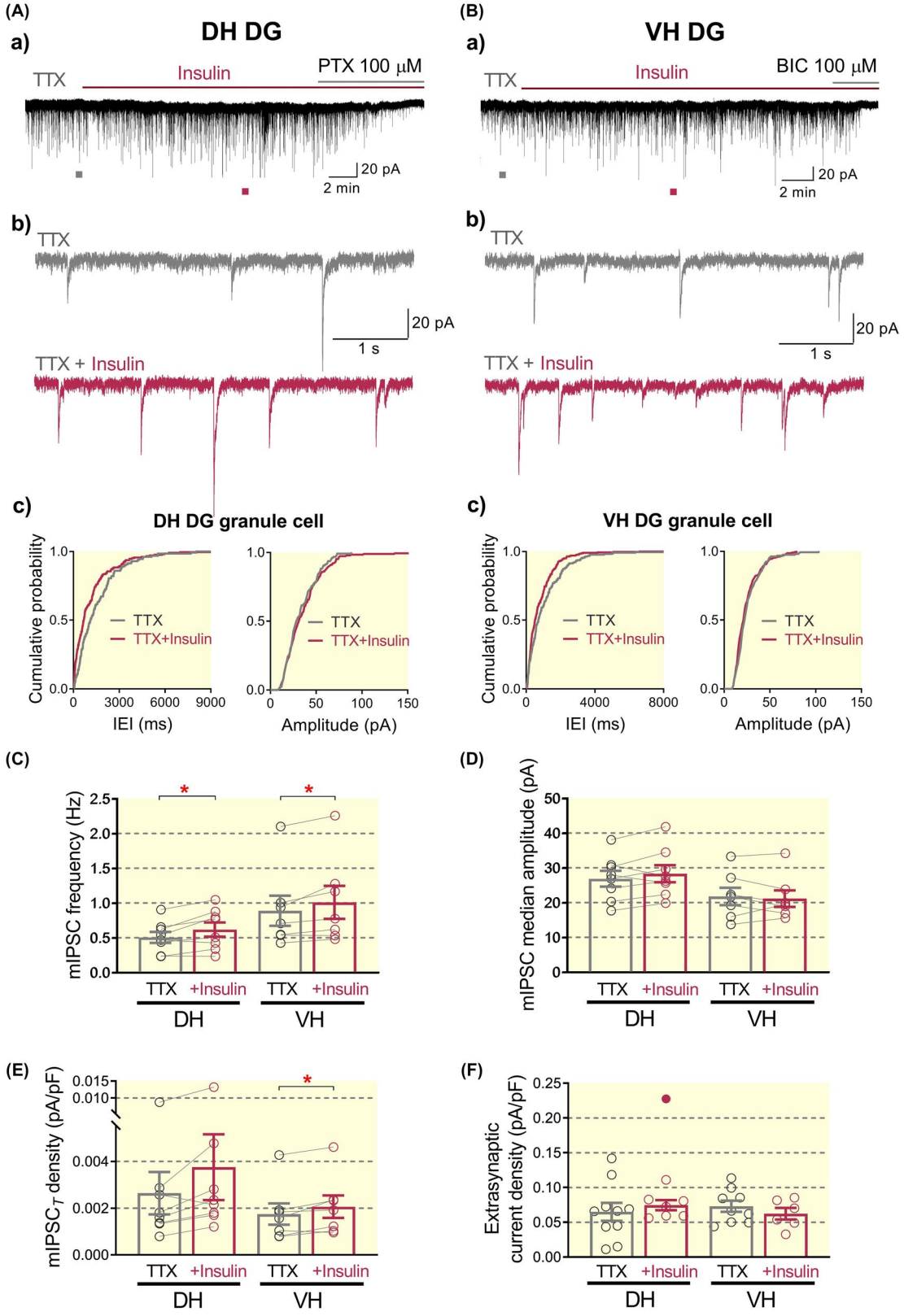

FIGURE 4 Insulin enhanced the GABAergic extrasynaptic current density in CA3 pyramidal neurons in the dorsal mouse hippocampus. Original records of $GABA_A$R-mediated currents from CA3 neurons of dorsal (DH, Aa) and ventral (VH, Ba) hippocampus under acute insulin (1 nmol/L) application. Upward shift of the baseline under the application of picrotoxin (PTX, 100 μmol/L) indicates the tonic current amplitude (as the difference between the dashed lines). The representative segments on expanded scale below the whole trace (marked with filled squares) depict sIPSCs under control (*ACSF, black trace*) and 1 nmol/L insulin application (*red trace*) recorded from CA3 pyramidal neuron of DH (Ab) and VH (Bb), respectively. Cumulative probability plots for the inter-event interval (IEI) and median amplitude of sIPSCs calculated from DH (Ac; from representative trace Aa) and VH (Bc; from representative trace Ba) CA3 neuron under control conditions (ACSF, *black line*) and insulin application (*red line*). The cumulative probability curves in control (ACSF, *black line*) and after bath perfusion of 1 nmol/L insulin (*red line*) did not indicate significant changes in the distribution of sIPSCs IEI and amplitude in CA3 pyramidal neuron in neither DH (Ac *left*; IEI, ACSF vs insulin: 305 vs 305 events analysed correspondingly; Ac *right*; Amplitude, ACSF vs insulin: 233 vs 239 events analysed respectively) nor VH (Bc *left*; IEI, ACSF vs insulin: 303 vs 302 events analysed; Bc *right*; Amplitude, ACSF vs insulin: 249 vs 248 events analysed correspondingly). Summary for the frequency (C), median amplitude (D) and total current density ($sIPSC_T$ density, E) of sIPSCs recorded from CA3 pyramidal neurons of DH (n = 9 neurons) and VH (n = 10 neurons) under control (*ACSF, black colour*) and insulin application (*red colour*). Summary statistics for extrasynaptic current density (F) in CA3 pyramidal neurons of DH (n = 6 neurons) and VH (n = 5 neurons) recorded under control conditions (*ACSF, black colour*) and after insulin application (*red colour*). Data are presented as dot plot for individual values and as bar plot for mean ± SEM. Connected lines indicate data obtained from individual neurons before (*black*) and during insulin application (*red*). Only statistically significant differences are marked on the graph. The Wilcoxon matched-pairs signed rank test, $*P < .05$. $V_{hold} = -60$ mV

similar in wild-type and the tg-APPSwe mice (Figure 7C-F; Figures S6 and S7A) and were not altered by insulin (Figure 7C-F). Since the DG granule cells vary in size (Figure 7G), we determined the median $sIPSC_T$ density and Figure 7H shows it is similar in the wild-type and the tg-APPSwe mice and not affected by insulin. In contrast, in the aged tg-APPSwe mice, insulin significantly modulated the sIPSCs. The sIPSCs frequency (Figure 8C) and $sIPSC_T$ (Figure 8F) were similar, in wild-type and the aged tg-APPSwe mice, but the sIPSCs amplitude (~14%, Figure 8D, Figure S6Bb), charge transfer (~16%, Figure 8E) and $sIPSC_T$ density (~33%, Figure 8H) decreased in the aged tg-APPSwe as compared to wild-type mice. Insulin did not modulate neither the IPSCs median amplitude (Figure 8D) nor the charge transfer (Figure 8E) in the aged animals but significantly enhanced the sIPSCs frequency (~51%, Figure 8C) and the median $sIPSC_T$ density (~58%, Figure 8H) but, importantly, only in the aged tg-APPSwe mice, resulting in normalized $sIPSC_T$ density and similar to wild-type values. The results indicate increased synaptic plasticity in the aged tg-APPSwe mice and is reminiscent of what was observed in the young, eight to ten weeks old wild-type mice.

2.2.2 | Insulin normalizes GABA-activated extrasynaptic current densities to wild-type levels in aged but not in 5-6 months old tg-APPSwe mice

The level of the GABA-activated extrasynaptic tonic current is relevant in the context of how control of baseline neuronal activity comes about. We measured the extrasynaptic tonic current amplitude in the presence or absence of insulin in the DG granule cells from 5 to 6 months old (Figure 9A) and aged (Figure 9B) mice. Typical current traces are shown in Figure 9Aa,b in the absence and presence of insulin for 5-6 months old wild-type and tg-APPSwe mice. There was a significant increase (~100%) in the extrasynaptic tonic current in the tg-APPSwe mice as compared with wild-type mice but insulin was without effect in both groups (Figure 9Ab,c). For the aged groups, typical current traces are shown in Figure 9Ba,b in the absence and presence of insulin. Interestingly, the increased (~100%) extrasynaptic tonic current was maintained in the aged tg-APPSwe as compared to wild-type mice (Figure 9Ba,c) but, importantly, insulin decreased the current and normalized the amplitude to similar levels as recorded in the wild-type mice (Figure 9Bb,c). The increased GABAergic tonic current was partially suppressed, 36 ± 16% (n = 3), by a selective inverse agonist, L-655,708 (100 nmol/L), in the aged tg-APPSwe mice. The results are consistent with the tonic extrasynaptic current in DG granule cells of aged tg-APPSwe mice is being mediated, in part, by $GABA_A$ receptors containing the α5 subunit, indicating that multiple $GABA_A$ receptors subtypes are involved in generating the conductance. The data demonstrate that the GABA-activated extrasynaptic tonic currents in DG granule cells are increased in tg-APPSwe mice, before and during amyloid plaques accumulation, as compared with the wild-type littermates. Insulin at near-physiological concentrations modulated the GABAergic signalling in the aged tg-APPSwe mice, demonstrating that the DG granule cells are not insulin resistant despite the amyloid pathology. Why insulin only normalized the currents in the aged mice remains to be clarified but implies increased plasticity in the aged tg-APPSwe mice.

2.2.3 | Insulin receptors are expressed in hippocampal DG granule cell layer of wild-type and tg-APPSwe mice

As we did not register any functional effects of insulin on GABA signalling in the wild-type mice, we examined if we could detect the IR in the DG granule cell layer

using immunohistochemistry and the results are shown in Figure S8. Substantial insulin receptor staining was detected in both wild-type and the tg-APPSwe mice at both 5-6 and 10-12 months of age when labelled with a primary antibody specific for the insulin receptor.

3 | DISCUSSION

Insulin is a metabolic hormone regulating peripheral glucose homeostasis but it is also increasingly acknowledged that insulin directly affects the brain by modulating neuronal

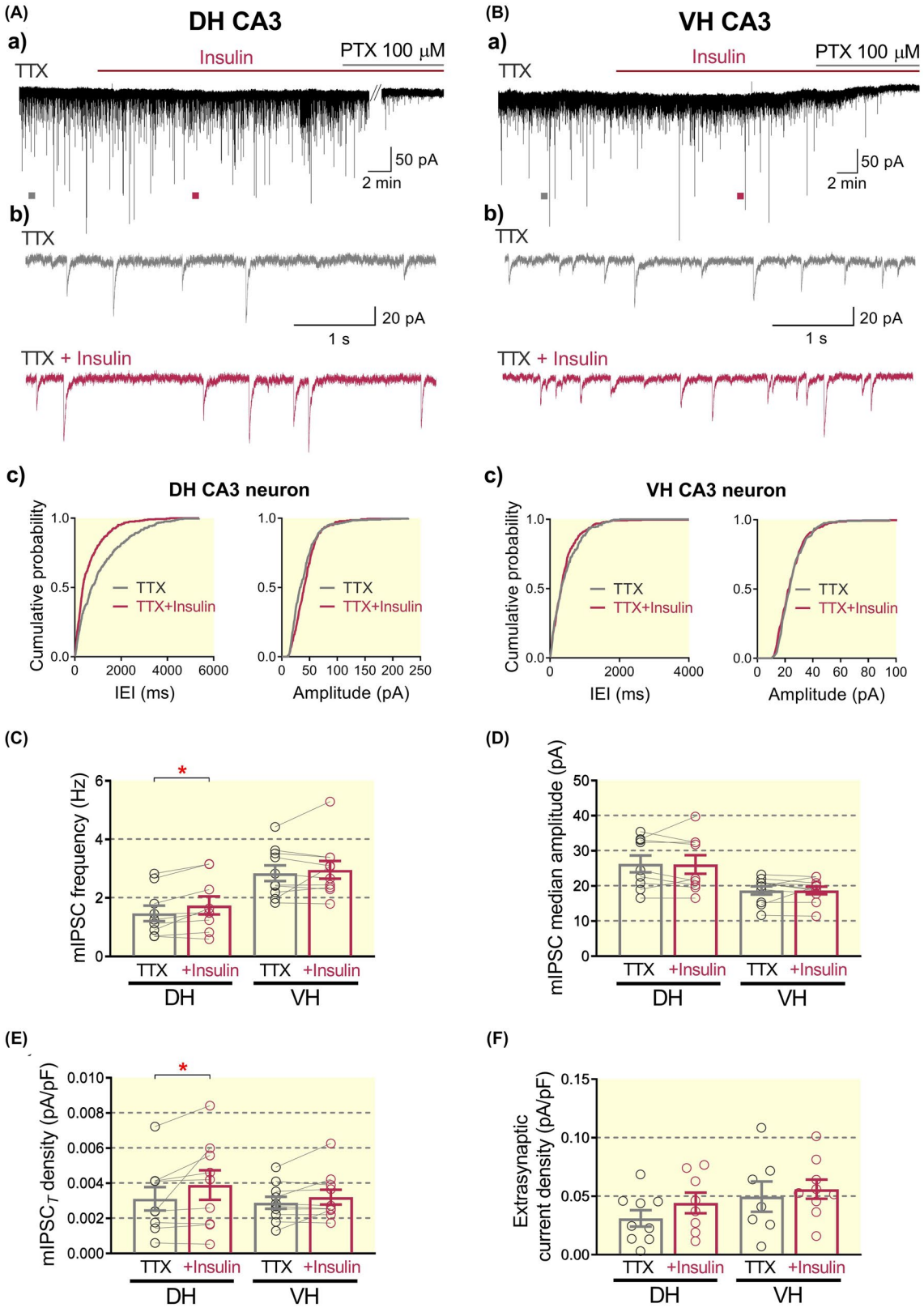

FIGURE 5 Insulin enhanced the frequency of the mIPSCs and $mIPSC_T$ density in CA3 pyramidal neurons in mouse dorsal hippocampus. Voltage-clamp recordings of mIPSCs and tonic currents in CA3 pyramidal neurons of DH (Aa) and VH (Ba) under 1 nmol/L insulin application. Marked regions with filled squares are shown on an expanded scale below the whole trace respectively. Trace segments on expanded scale represent mIPSCs from CA3 neuron from mouse DH (Ab) and VH (Bb) respectively under control (TTX, *grey trace*) conditions and during insulin application (*dark red trace*). Miniature IPSCs were recorded in the continuous presence of TTX (1 μmol/L). Examples of cumulative probability plots for the inter-event interval (IEI) and median amplitude of mIPSCs from DH (Ac; from representative trace Aa) and VH (Bc; from representative trace Ba) CA3 neuron under control (TTX, *gray line*) and 1 nmol/L insulin application (TTX + insulin, *dark red line*). The left shift of the cumulative probability curve after insulin perfusion (*dark red line*) indicates a decrease in mIPSCs IEI (that corresponds to increased mIPSCs frequency) in CA3 neuron of DH (Ac *left*; IEI; TTX vs TTX + insulin: 339 vs 330 events analysed correspondingly) but not in VH (Bc *left*; IEI; TTX vs TTX + insulin: 300 vs 360 events analysed correspondingly). The cumulative distribution plots for mIPSCs amplitude in control (TTX, *gray line*) and under insulin application (*dark red line*) did not indicate significant changes in the distribution of mIPSCs amplitude in CA3 pyramidal neuron in neither DH (Ac *right*; Amplitude; TTX vs TTX + insulin: 316 vs 294 events analysed correspondingly) nor VH (Bc *left*; Amplitude; TTX vs TTX + insulin: 252 vs 303 events analysed correspondingly). Summary for the frequency (C), median amplitude (D) and total current density ($mIPSC_T$ density, E) of mIPSCs recorded from CA3 pyramidal neurons of DH (n = 9 neurons) and VH (n = 10 neurons) under control (TTX, *gray colour*) and bath application of insulin (*dark red colour*). Summary statistics for extrasynaptic current density (F) in CA3 pyramidal neurons of DH (8-9 neurons) and VH (7-9 neurons) recorded in the presence of TTX under control conditions (*TTX, gray colour*) and after insulin application (*dark red colour*). Data are presented as dot plot for individual values and bar plot for mean ± SEM. Connected lines indicate data obtained from individual neurons before (*gray*) and during insulin application (*dark red*). Only statistically significant differences are marked on the graph. The Wilcoxon matched-pairs signed rank test/non-parametric Mann-Whitney *U* test, $*P < .05$. $V_{hold} = -60$ mV

plasticity and function.[3,10] Here, we examined the effects of insulin on the tonic GABA-activated currents in primary neurons of the characteristic neuronal network module that is repeated in a parallel lamellar fashion along the longitudinal axis of the hippocampus. We used insulin at near-physiological concentration (1 nmol/L) in order to selectively activate its cognate receptors.[44,56] The results demonstrate that in young, 8-10 weeks old mice, insulin regulates the tonic GABA-activated synaptic and extrasynaptic current density in DG granule cells and CA3 pyramidal neurons, according to cell-type and position along hippocampal dorsoventral axis (Figure 10A) and is consistent with the reported ability of insulin to reduce spontaneous neuronal firing. This in contrast, to the results from the dorsal DG granule cells from older (5-12 months old) wild-type mice where insulin was without effects. However, in the dorsal DG granule cells from tg-APPSwe mice, the insulin modulation was related to age and progression of the disease (Figure 10B). The results indicate that insulin regulates GABA signalling when neuronal networks are changing, as happens during maturation of the young brain[3,29] and as the disease progresses in the hippocampus of the aged tg-APPSwe mice.[38,62]

It is well-established that the hippocampus is a brain structure essential for formation of spatial memory, navigation and emotional responses.[53,55] What is less appreciated is that the hippocampus has receptors for insulin and a number of other metabolic hormones and participates in sensing and regulating body physiology by modulating, in a topographical manner, activity of hypothalamic neurons.[5,63] The hippocampus is a long, curved structure with a longitudinal axis ranging from dorsal (septal)-to-ventral (temporal) in rodents and corresponds to the posterior-to-anterior hippocampus in humans.[53,55,64] The dorsal hippocampus receives information from the sensory cortices whereas the ventral hippocampus has more connectivity with the hypothalamus, amygdala and prefrontal cortex.[55,63,65-67] According to common simplification of the endogenous diversification of the hippocampus, we divided the structure along the dorsoventral axis into dorsal, intermediate and ventral domains[53,55] and studied the effects of insulin on the dorsal and ventral DG granule cells and CA3 pyramidal neurons.

The insulin receptor was prominently expressed in the granule cell layer and the CA3 pyramidal neuronal layer both in the dorsal and ventral hippocampus. It was, therefore, somewhat surprising that the effects of insulin on GABA signalling in the neurons varied both with location and with age. In the young mice, in the DG granule cells, insulin increased the sIPSC frequency and current density in the dorsal and ventral neurons but the effect on the current density, in the absence of action potentials, was only maintained in the ventral DG granule cells. The increase in sIPSC amplitude observed in the dorsal DG granule cells, was not maintained in TTX and no effect of insulin was recorded for the extrasynaptic current. These results are in agreements with no effect of insulin on the postsynaptic $GABA_A$ receptors in the DG granule cells and, further, are consistent with insulin-enhanced presynaptic GABA release and stronger effects of insulin in the ventral DG areas of the hippocampus. In the CA3 pyramidal neurons, insulin only enhanced the extrasynaptic current density in the dorsal hippocampus, which was lost in TTX where, on the other hand, an increase in mIPSC frequency and the resulting increased mIPSC density was revealed. Similar to the DG granule cells, the effects of insulin can be attributed to presynaptic mechanisms and the increase in the extrasynaptic current, that was lost in TTX, suggests increased spillover of GABA from synapses in the presence of action potentials and insulin. It is interesting that only GABA-activated currents in the ventral CA3 pyramidal neurons appear to be insensitive to

insulin. We previously reported that these neurons normally have a weak, basal GABAergic inhibitory tone.[29] The present results show that insulin, an innate modulator of GABA signalling, does not enhance the GABAergic system in these neurons. What advantage this offers physiologically is not clear, but is relevant in relation to the observation that the ventral hippocampus is more prone to epileptic activity than the dorsal hippocampus.[47,49,51-54] As insulin does not enhance the inhibition in the ventral CA3 pyramidal neurons, it does not alter the excitability or the propensity to epileptic activity

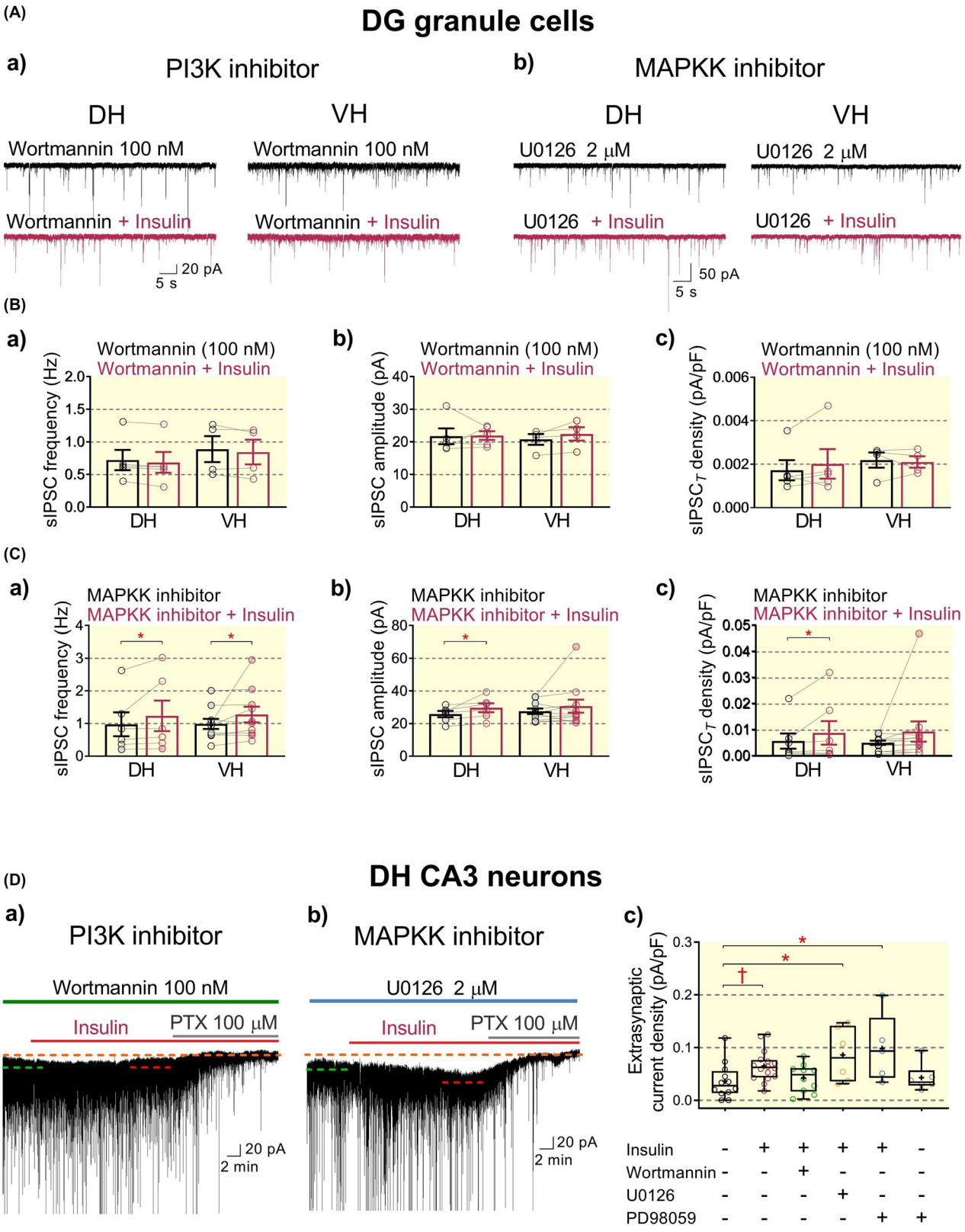

FIGURE 6 Wortmannin eliminated insulin-induced enhancement of $GABA_A$ receptors-mediated currents in dentate gyrus granule cells and CA3 pyramidal neurons in the mouse hippocampus. (Aa) Representative recordings of GABAergic currents from DG granule cells of dorsal (DH) and ventral (VH) under wortmannin (100 nmol/L, *top black traces*) pretreatment following acute insulin application (1 nmol/L) in the constant presence of 100 nmol/L wortmannin (*below, red traces*). (Ab) Representative traces of GABAergic currents from DG granule cells of DH and VH under U0126 (2 μmol/L) pretreatment (*top, black colour*) following acute insulin application (1 nmol/L) in the constant presence of 2 μmol/L U0126 (*below, red traces*). Summary statistics of sIPSC frequency (Ba), median amplitude (Bb) and total synaptic current ($sIPSC_T$) density (Bc) recorded from DG granule cells of DH (n = 5 cells) and VH (n = 4 cells) under continuous 100 nmol/L wortmannin treatment (*black colour*) and 1 nmol/L insulin application in the presence of wortmannin (*red colour*). (Ab, C) MAPKK inhibition does not eliminate insulin-induced enhancement of synaptic $GABA_A$ receptor-mediated currents in DG granule cells in DH and VH. Summary statistics of the frequency (Ca), median amplitude (Cb) and $sIPSC_T$ density (Cc) of sIPSC recorded from DG granule cells of DH (n = 7 cells) and VH (n = 11 cells) under 2 μmol/L U0126 (*filled circles*) or 20 μmol/L PD98059 (*opened circles*) treatment (MAPKK inhibitor*; black colour*) and 1 nmol/L insulin application in the constant presence of U0126 (*filled circles*) or PD98059 (*opened circles*) (MAPKK inhibitor + insulin; *red colour*). Data is presented as dot plot for individual values and bar plot for mean ± SEM. Connected lines indicate data obtained from individual neurons before (*black*) and during insulin perfusion *(red*). (D) Wortmannin, but not PD98059 inhibits insulin-induced potentiation of extrasynaptic $GABA_A$ receptor-mediated currents in CA3 pyramidal neurons in DH. (Da) Representative trace demonstrating that bath application of 1 nmol/L insulin does not alter the magnitude of extrasynaptic currents recorded from CA3 pyramidal neurons in the presence of 100 nmol/L wortmannin. (Db) Original record shows that the insulin-induced potentiation of the current was preserved in the presence of 20 μmol/L PD98059. Upward shift of the baseline under the application of picrotoxin (PTX, 100 μmol/L) indicates the current amplitude (as the difference between the dashed lines). (Dc) Compiled data showing the extrasynaptic current density under basal conditions (n = 12 neurons) and after insulin application in the presence of 100 nmol/L wortmannin (n = 10 neurons) or 2 μmol/L U0126 (n = 6 neurons) or 20 μmol/L PD98059 (n = 5 neurons). Data is presented as a scatter dot plot with a box and whiskers plot with median values plotted by the Tukey method and mean values shown as '+'. Only statistically significant differences are marked on the graph. The Wilcoxon matched-pairs signed rank test/non-parametric Mann-Whitney *U* test, $^*P < .05$, $^\dagger P < .01$. $V_{hold} = -60$ mV

of this region by modulating the GABAergic system in these neurons. However, maintaining a set inhibitory tone may be imperative to preserve a more conserved homeostatic metabolic regulatory role of the hypothalamic nuclei by the ventral hippocampus.[5,63]

Previous studies of insulin effects on GABA-activated currents in cultured rat hippocampal neurons,[68,69] rat dorsal CA1 pyramidal neurons,[44] rat prefrontal cortex[70] and mouse cerebellar granule cells[71] have shown that insulin strengthens GABAergic signalling by inserting or turning-on new $GABA_A$ receptors in the postsynaptic neurons. In the current study, in the absence of action potentials in the young mice, insulin increased the frequency of synaptic events in the dorsal and ventral DG granule cells and the dorsal CA3 pyramidal neurons whereas no effect was observed on the synaptic median amplitude or extrasynaptic currents, consistent with insulin enhancing presynaptic release of GABA. Insulin increased the mIPSC frequency/density revealing a slight effect on the dorsal CA3 pyramidal neurons IPSCs that was not observed for the sIPSCs. This increase may, nevertheless, have contributed to the greater extrasynaptic current density in the dorsal CA3 pyramidal neurons in the presence of insulin, resulting from more interstitial GABA originating from spillover of GABA from the synapses. In the absence of insulin, the level of the extrasynaptic current was similar in the presence or absence of action potentials.[29] Together the results indicate that the normally low extrasynaptic current in the dorsal CA3 pyramidal neurons will become larger with increased synaptic activity and GABA spillover from synapses.

The IR was expressed in the DG granule cell layer irrespective of age or animal model. It was, therefore, somewhat surprising that the effects of insulin in the older mice on GABA signalling were only manifested in the aged tg-APPSwe mice. In the 5-12 months wild-type and 5-6 months tg-APPSwe mice, insulin did not modulate the sIPSCs or the extrasynaptic current density. In contrast, in the aged tg-APPSwe mice, insulin increased the sIPSCs density but decreased the extrasynaptic current density. This is particularly interesting as in the aged tg-APPSwe mice, the sIPSCs density was significantly decreased relative to the values recorded in aged wild-type mice. Furthermore, in the 5-6 months old tg-APPSwe mice, the extrasynaptic current density was significantly increased relative to the wild-type mice and, this increase was maintained in the older tg-APPSwe mice. However, in the 5-6 months old tg-APPSwe mice insulin had no effect whereas in the aged tg-APPSwe mice, insulin decreased and normalized the extrasynaptic current density to wild-type levels. In tg-APPSwe mice intraneuronal Aβ aggregation is observed at 6 months of age[60] and extracellular plaque deposition, microgliosis and astrogliosis are detected in the hippocampus at 12 months of age.[59,60] In this study, no Aβ plaques were observed in the 5-6 months tg-APPSwe mice but were present in the aged tg-APPSwe mice, in agreement with the previous reports.[59,60] The GABA signalling was thus already changing in the 5-6 months old tg-APPSwe mice, but, only in the aged tg-APPSwe animals were the insulin modulating-mechanisms in place. That the sIPSCs amplitudes and densities were decreased in the aged tg-APPSwe mice relative to the aged wild-type littermates, implies a general decrease in the number of postsynaptic $GABA_A$ receptors in the DG granule cells in the aged tg-APPSwe animals or, alternatively, decreased release of GABA from the presynaptic terminals. It is possible that the increased tonic current that was normalized by insulin is related, in part, to the synaptic-type

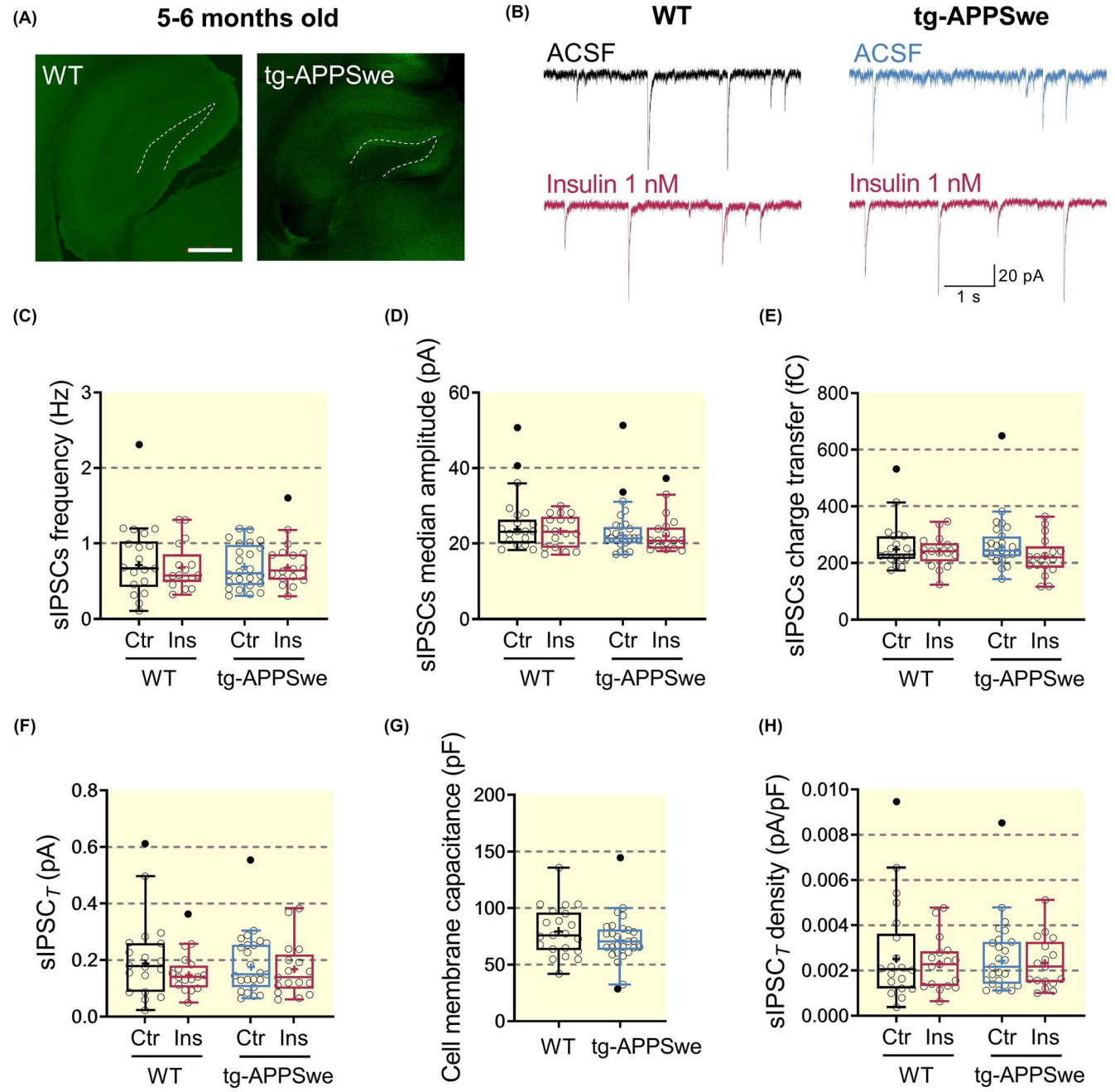

FIGURE 7 Insulin does not modulate fast spontaneous IPSCs in dentate gyrus granule cells of the dorsal hippocampus in 5-6 mo old tg-APPSwe mice and wild-type (WT) littermates. A, Representative images of Thioflavin S staining in the hippocampus of 5-6 mo old wild-type (WT) and tg-APPSwe mice: no plaques were detected in the DG region. Dashed line indicates DG granule cell layer (Scale bar 500 μm). B, Voltage-clamp recordings of sIPSCs in DG granule cells of dorsal hippocampus from 5 to 6 mo old wild-type and tg-APPSwe mice under control conditions (ACSF, *black/blue traces, upper panel*) and insulin (1 nmol/L) pre-incubation (*red traces, below panel*). Summary for the mean frequency (C) the median amplitude (D), the median charge transfer (E) and the total synaptic current (sIPSC$_T$, F) of sIPSCs in DG granule cells of wild-type and tg-APPSwe mice (5-6 mo old) recorded from dorsal hippocampal slices under control conditions (Ctr, *black/blue*) and after pre-incubation with 1 nmol/L insulin (Ins, *red*). G, The dorsal DG granule cell membrane capacitances were similar between WT and tg-APPSwe mice (5-6 mo old) under control conditions (ACSF). H, Summary plot for the total synaptic current density (sIPSC$_T$ density) of sIPSCs in DG granule cells of WT and tg-APPSwe 5-6 mo old mice. Data are presented as scatter dot plot for individual values and box and whiskers plot with median value plotted as a line and mean value shown as '+'. Outliers were defined by the Tukey method and are marked as dot plot (*filled black circles*) and excluded from the statistical analyses. Non-parametric Mann-Whitney *U* test (two-tailed). All experiments were performed with parallel controls from the same animal/age group. $V_{hold} = -60$ mV

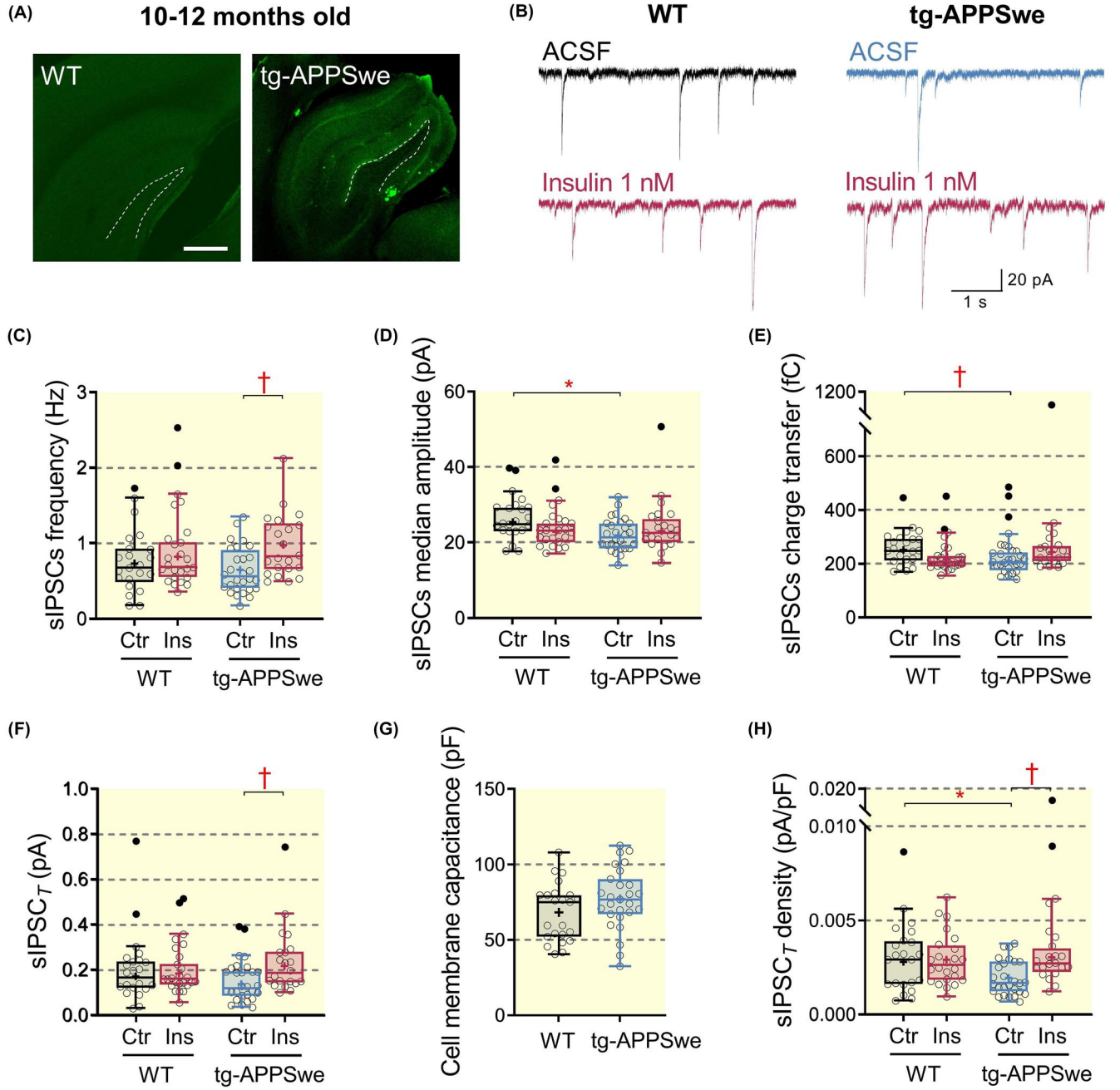

FIGURE 8 Insulin modulates fast spontaneous IPSCs in dentate gyrus granule cells of the dorsal hippocampus in 10-12 mo old tg-APPSwe mice but not wild-type (WT) littermates. A, Microphotographs of Thioflavin S staining of neuritic plaques (*bright green*) in the hippocampus of tg-APPSwe and wild-type 10-12 mo old mice. It is shown that the most plaques are deposited in the DG region in aged (10-12 mo) tg-APPSwe AD mouse model. No plaques were detected in the hippocampus of wild-type littermates. Dashed line indicates DG granule cell layer (Scale bar 500 μm). B, Original traces of sIPSCs recorded from dorsal DG granule cells of 10-12 mo old wild-type and tg-APPSwe mice under control conditions (ACSF, *black/blue traces, upper panel*) and insulin (1 nmol/L) pre-incubation (*red traces, below panel*). Summary graphs for the mean frequency (C), the median amplitude (D), the median charge transfer (E), the total synaptic current (sIPSC$_T$, F) and the total synaptic current density (sIPSC$_T$ density, H) of sIPSCs recorded from DG granule cells of dorsal hippocampal slices from WT and tg-APPSwe mice (10-12 mo old) under control conditions (Ctr, *black/blue*) and after pre-incubation with 1nmol/L insulin (Ins, *red*). G, The cell membrane capacitances were similar between dorsal DG granule cell of WT and tg-APPSwe 10-12 mo old mice (in ACSF). Data are presented as scatter dot plot for individual values and box and whiskers plot with median value plotted as a line and mean values shown as '+'. Outliers were detected by the Tukey method and marked as dot plot (*filled black circles*) and excluded from the statistical analyses. Only statistically significant differences are marked on the graph. Non-parametric Mann-Whitney *U* test (two-tailed); $^{*}P < .05$, $^{\dagger}P < .01$. All experiments were performed with parallel controls from the same animal/age group. $V_{hold} = -60$ mV

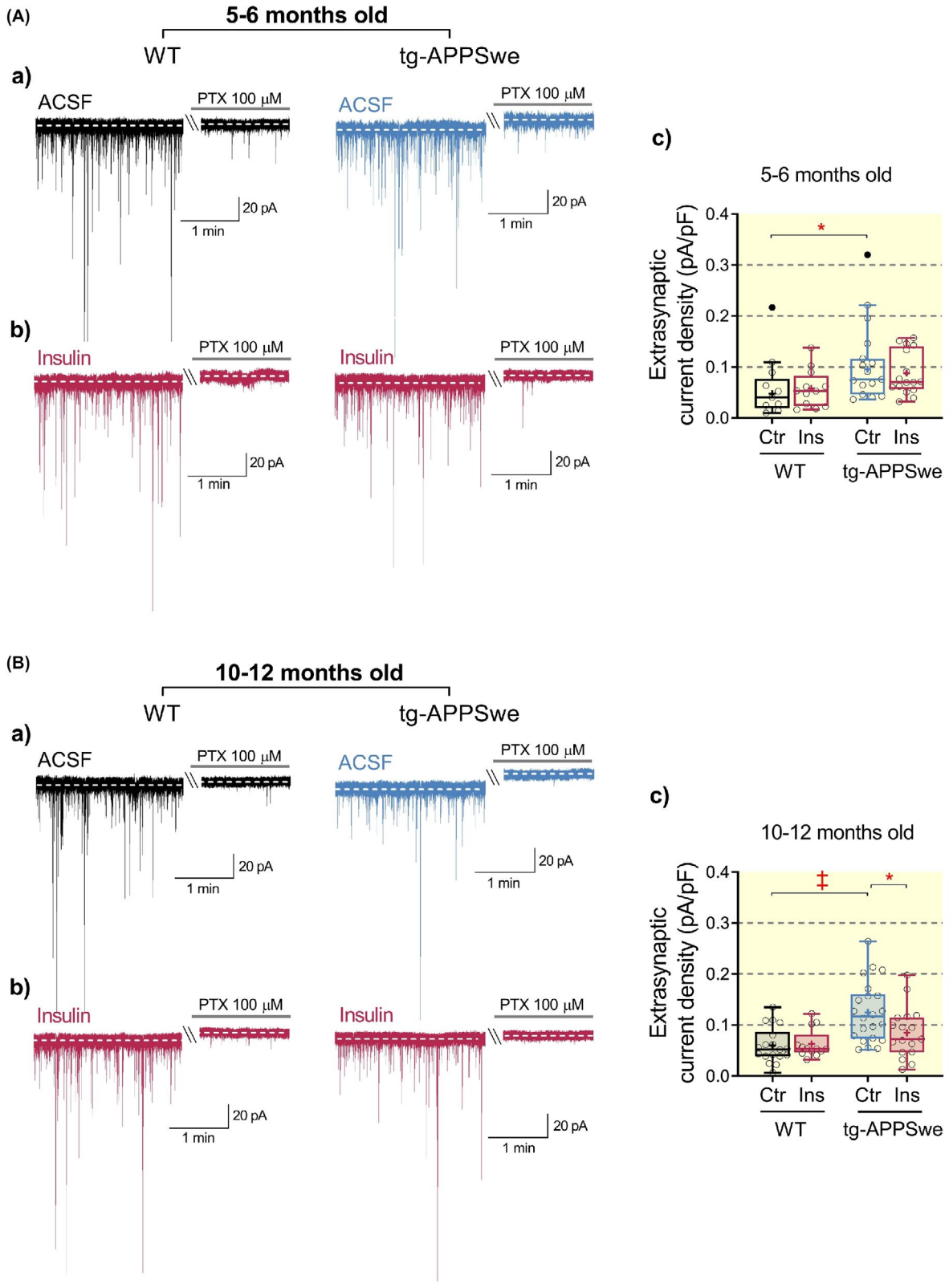

receptors remaining outside of synapses in the aged tg-APPSwe mice but then, are rescued by insulin, resulting in normalized and increased synaptic and decreased extrasynaptic current densities.[72-74] Notably, the DG granule cells are clearly not insulin resistant in the presence of amyloid pathology. A prominent feature in AD is accumulation of Aβ peptides in the brain, sometimes decades before onset of cognitive symptoms.[60,75] The net increase in neuronal excitatory/inhibitory ratio observed in mouse models of AD is thought to be linked to the association of Aβ to synapses resulting in

FIGURE 9 Effect of insulin on GABA-activated extrasynaptic current density in dentate granule cells in 5-6 and 10-12 mo old wild-type and tg-APPSwe mice. A, Insulin does not modulate GABA-evoked extrasynaptic tonic currents in dorsal dentate granule cells in 5-6 mo old tg-APPSwe mice and wild-type (WT) littermates. Representative voltage-clamp recordings of sIPSCs and extrasynaptic tonic currents in DG granule cells from adult (5-6 mo or months) wild-type and tg-APPS we mice under control conditions (Aa, ACSF, *black/blue*, Ctr) and after 1 nmol/L insulin exposure (Ab, Insulin, *red*, Ins). The tonic current was revealed by blocking $GABA_A$ receptors with picrotoxin (PTX, 100 µmol/L) resulting in shift of the baseline current. The extrasynaptic tonic current amplitude was significantly higher in the tg-APPSwe mice when compared with wild-type littermates. (Ac) The GABA-evoked extrasynaptic tonic current density in DG granule cells of wild-type and tg-APPSwe mice (5-6 mo old) under control conditions (Ctr, *black/blue*) and after pre-incubation with 1 nmol/L insulin (Ins, *red*). The density of the tonic extrasynaptic GABA-activated current was measured by dividing current amplitude (pA) by the cell membrane capacitance (pF). B, Insulin normalizes increased tonic GABA-activated extrasynaptic current density in dentate granule cells in 10-12 mo old tg-APPSwe mice. Representative inhibitory current traces from DG granule cells from dorsal hippocampal slices from 10 to 12 mo old wild-type and tg-APPSwe mice under control conditions (Ba, ACSF, *black/blue*, Ctr) and after exposure to 1 nmol/L insulin (Bb, Insulin, *red*, Ins). Upward shift of the baseline under the application of picrotoxin (PTX, 100 µmol/L) identifies the tonic current amplitude (as the difference between the dashed lines). The tonic extrasynaptic current amplitude was significantly higher in tg-APPSwe mice when compared with the wild-type littermates. (Bc) Data showing the extrasynaptic current density in DG granule cells from wild-type and tg-APPSwe mice (10-12 mo old) under basal conditions (Ctr, *black/blue*) and after pre-incubation with 1 nmol/L insulin (Ins, *red*). Data are presented as scatter dot plot for individual values and box and whiskers plot with median values plotted as lines and the mean values shown as '+'. Outliers are detected by the Tukey method and marked as dot plot (*filled black circles*). Statistical analyses are performed by excluding outliers and only statistically significant differences are marked on the graph. For statistical analysis the Mann-Whitney *U* test (two-tailed) was used. Significance levels are $^{*}P < .05$, $^{\ddagger}P < .001$. All experiments were performed with parallel controls from the same animal/age group. $V_{hold} = -60$ mV

FIGURE 10 Schematic summary. A, The schematic drawing illustrates the effects of insulin (1 nmol/L) on GABA-activated tonic current densities in hippocampal neurons along the dorsoventral axis. Positioning of the patch-clamp electrodes identifies relevant recording hippocampal areas. DH: dorsal hippocampus, VH: ventral hippocampus, DG: dentate gyrus. -TTX: in the absence of TTX, +TTX: in the presence of TTX. B, The schematic drawing depicts the effects of 1 nmol/L insulin on GABA-activated tonic current densities in dorsal hippocampal DG granule cells in wild-type and tg-APPSwe mice at 5-6 and 10-12 mo of age. Positioning of the patch-clamp electrodes identifies the DG hippocampal area where the recordings were made. -Insulin: in the absence of insulin, +Insulin: in the presence of insulin

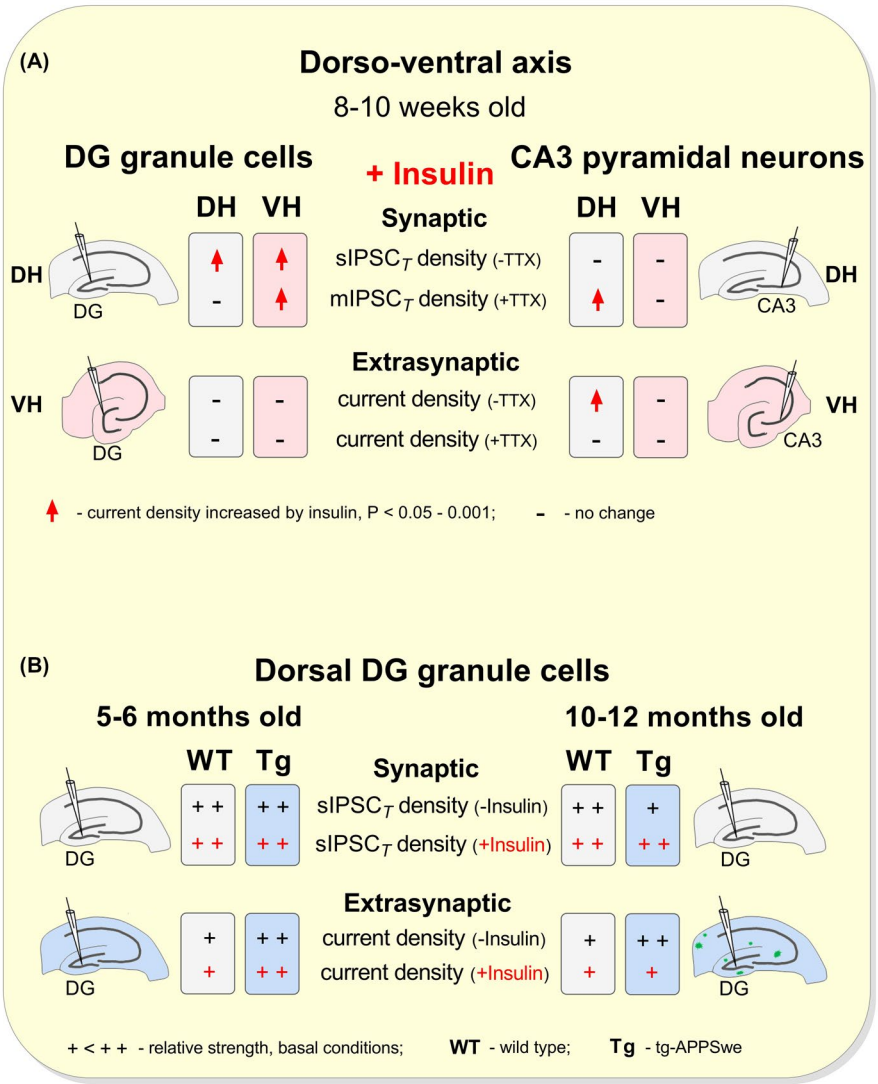

impaired synaptic and network activity.[37,38,62] Our observation of decreased $sIPSC_T$ density in aged tg-APPSwe mice as compared to wild-type littermates confirms the decreased inhibitory synaptic tone in tg-APPSwe mice but also, and importantly, demonstrates how the inhibitory transmission can be rescued by insulin.

The $GABA_A$ receptors have been shown to be well-preserved in the hippocampus of aged mice[76] and this observation is in agreement with the robust and similar GABA signalling we observed in the DG granule cells from ~2,[29] 5-6 and 10-12 months old wild-type mice. Alterations in expression of $GABA_A$ subunits and the receptor subtypes might nevertheless take place as the disease progresses and contribute to the changes we observe in the tg-APPSwe mice.[77-83] Increased extrasynaptic GABA-activated hippocampal currents, as we recorded in the 5-12 months old tg-APPSwe mice, has been associated with memory modulation[84,85] and our results, from the 8-10 weeks old DG granule cells and previously from rat CA1 pyramidal neurons,[44] demonstrate that insulin can increase extrasynaptic GABA-activated currents. In contrast, the results from the aged tg-APPSwe DG granule cells herein revealed that insulin regulation can also enable return to normal wild-type values. Insulin regulation of GABA signalling in hippocampal neurons thus appears to be multifaceted and critically context-based.

Insulin potentiation of the synaptic and extrasynaptic currents in the present study was PI3K-signalling dependent. It is well-established that insulin can evoke PI3K signalling in many types of cells modulating trafficking of proteins leading to altered transmitter release[86,87] or insertion of transporters or ion channels, including $GABA_A$ receptors, into the plasma membrane.[44,69,70,88] In the aged tg-APPSwe mice, the results are consistent with the extrasynaptic current, in the dorsal DG granule cells, being mediated in part by $GABA_A$ receptors containing the α5 subunit. This is interesting as insulin has previously been demonstrated, in rat hippocampal CA1 neurons, to regulate extrasynaptic GABA-activated currents by altering the prominence of α5-containing $GABA_A$ receptors by a PI3K-dependent signalling.[44]

The GABAergic interneurons have a crucial role in regulating the hippocampal networks, including the hormonal effects,[89,90] and this is clearly in accordance with the results presented herein. The differences in density, spatial distribution and connectivity of GABAergic neurons along the dorsoventral axis of the hippocampus have been well-described.[89,90] The spatial distribution of GABAergic contacts is similar for the different parts of the CA3 pyramidal neurons but more focused on the granule cell somata in the dentate gyrus.[89,90] The dorsal hippocampus receives information from sensory cortices whereas the ventral hippocampus has more connectivity with the hypothalamus, amygdala and prefrontal cortex.[55,63] The hippocampus then participates in formation of spatial memories, navigation and emotional responses,[53,55] in addition to its less-well-known role in regulating general body physiology and behaviour.[5,63] The current study highlights how selective, but still multifaceted, the insulin effect can be in neurons. Not only is the response to insulin related to the cell-type, the hippocampal axis-location of the cells, age of the animals and disease but also to the subtype of neuronal inhibition involved, synaptic or extrasynaptic $GABA_A$ receptors-activated currents.

Increasing evidence indicates that insulin normally facilitates a number of brain functions including motivation and cognition[3] and, insulin has been indicated in having a protective role in relation to the progressive pathogenesis of AD.[2,17] Insulin dysfunction, on the other hand, is the principal hallmark of type 2 diabetes mellitus[91] and metabolic dysregulation is a risk factor for cognitive decline, vascular dementia and AD.[91-94] Our current and previous results on the GABA signalling system in the hippocampus[29,44] and others on the glutamatergic system (see Ref.3 and references there within), support the concept that the insulin effects are a critical part of normal development, plasticity and homeostasis in the hippocampus in health and disease. It is possible that when gradual changes in hippocampal function are taking place, normal physiology may be maintained or recovered in eg type 2 diabetes mellitus or AD, by metabolic hormones, like insulin. In cases where insulin sensitivity is decreased, other metabolic hormones that evoke PI3K signalling, eg GLP-1 and its mimetics, may potentially function as a substitute and partially recover normal function.[95] Whether insulin has a role in other brain diseases, eg psychiatric diseases, remains to be explored but considering the wide distribution of the insulin receptor in the brain,[3,96] it seems likely that normal insulin signalling is of importance for healthy brain function and may serve to normalize imbalances in a range of brain pathologies.

4 | CONCLUSIONS

In the hippocampus of young mice, insulin modulated signalling at inhibitory synapses and extrasynaptic $GABA_A$ receptors by enhancing the basal GABA-activated currents. The outcome of the insulin modulation was dependent on the neuronal subtype and the hippocampal longitudinal axis-location of the neuron. In contrast, insulin did not modulate GABA signalling in healthy adult (5-6 months) or aged (10-12 months) wild-type mice. However, in transgenic mice with the Swedish mutation (tg-APPSwe), an AD mouse model, an increase in the GABA-evoked extrasynaptic current density developed in the hippocampal dorsal DG granule cells and, in addition, the synaptic current densities decreased in the aged tg-APPSwe mice. Importantly, insulin at near-physiological concentrations (1 nmol/L) normalized the currents to wild-type values in the aged tg-APPSwe mice. The current results contribute to the understanding of how insulin by selective facilitation of GABA-activated currents alters

neuronal excitability in specific principal hippocampal neurons and, thereby, hippocampal function in the developing or the changing brain. The results support the view that insulin in the hippocampus promotes and maintains normal function of the neurons.

5 | MATERIAL AND METHODS

5.1 | Animals

All experiments were performed in accordance with the local ethical guidelines and protocols approved by Uppsala animal ethical committee, Swedish law and regulations based on the Directive 2010/63/EU.

5.2 | Young mice

Eight to ten weeks old C57BL6J male mice (Taconic M&B, Denmark), were used in dorsoventral axis experiments. For the DG granule cells, hippocampal slices from 53 mice were used to record from dorsal hippocampus (DH, 22 mice) and ventral hippocampus (VH, 31 mice). For the CA3 pyramidal neurons, hippocampal slices from 80 mice were used to record from DH (67 mice) and VH (24 mice) and four mice were used for immunohistochemistry.

5.3 | Adult mice

Adult (5-6 months old) and aged (10-12 months old) male and female C57BL6 and tg-APPSwe (bred on a C57/BL6 background) mice were used in these experiments. Male and female tg-APPSwe mice were bred at Uppsala University by crossing male heterozygous tg-APPSwe with female C57BL6. Age-matched male and female C57BL6 mice were used as wild-type controls. Mice were maintained in a 12 h light/12-h dark cycle with water and food *ad libitum*. Efforts were made to reduce the number of animals used in experiments. In total, 36 hippocampal slices were used from 6 WT 5-6 months old mice, 41 slices - from 7 tg-APPSwe 5-6 months old mice, 47 slices - from 8 WT 10-12 months old mice and 50 slices - from 13 tg-APPSwe 10-12 months old mice to record GABA-activated currents from DG granule cells of dorsal hippocampus. Activity of one neuron was recorded from each slice.

5.4 | Genotyping

Tg-APPSwe mice overexpress transgene with human APP (isoform 695) bearing the Swedish mutation (KM670/671NL) under the murine Thy1 promoter.[60] In order to detect the presence of the expected gene we used fast genomic DNA isolation method ´HotSHOT´ from mouse tail tip.[97] In brief, alkaline lysis solution (25 mmol/L NaOH, 0.2 mmol/L Na_2EDTA, pH around 12) was added to the tissue samples and then heated at 95°C for 45 minutes followed by cooling to 4°C. After, the neutralizing buffer (40 mmol/L Tris-HCl, pH around 5) was added to each sample and mixed briefly. We prepared a PCR master mix with JumpStart™ Taq DNA Polymerase (Catalog Number D6558, Sigma-Aldrich) and added primer pair (APP –TYI-1-GAATCCAAGTCGGAACTCTT; APP-SQ6rw-TGTCAGGAACGAGAAGGGCA) to run the PCR reaction using the cycling parameters following the initial heating at 94°C (2 minutes): 94°C (15 seconds), 63°C (15 seconds), 72°C (30 seconds) for 30 cycles and then incubation at 72°C (10 minutes). The samples were further subjected to electrophoresis on a 1% agarose gel and the expected PCR product sizes were 400 bp (Figure S9).

5.5 | Brain tissue collection and fixation for immunohistochemistry

5.5.1 | Young mice

Animals (8-10 weeks old) were anaesthetized by intraperitoneal injection of 0.2 mL Dormitor (1 mg/mL, OrionPharma, Danderyd, Sweden) and 0.2 mL Ketalar (10 mg/mL, Pfizer, Kent, UK). The brain was dissected out after transcardiac perfusion using ice-cold 0.1 mol/L phosphate buffered saline (PBS) followed by 4% formaldehyde solution (FA, Histolab, Askim, Sweden). The hippocampus was separated from surrounding tissue, placed in a 4% agarose gel (Cambrex Bio Science, ME, USA) and fixed by 4% FA for 3 hours on ice. After washing with PBS, the tissue was immersed at 4°C overnight, first in 20% and then in 30% sucrose in 0.1 mol/L PBS (pH = 7.4). The hippocampus was divided into dorsal and ventral parts and then frozen in cryo-protective medium Neg-50 (Thermo Fisher Scientific, USA).

5.5.2 | Adult mice

After the first 3-4 hippocampal slices (coronal sections) from dorsal pole of each hemisphere were sliced and collected for electrophysiological experiments, the remaining brain tissue was carefully unglued from the platform and immersed into 4% FA (Histolab, Askim, Sweden). As described previously, the fixation lasted for 3 hours in 4% FA on ice. Then, the brain tissue was washed with 0.1 mol/L PBS (pH = 7.4) followed by sequential immersion in 20% and 30% sucrose solution in 0.1 mol/L PBS (4°C; overnight). The hemispheres were further frozen in OCT mounting medium (VWR Chemicals, UK).

5.5.3 | Immunohistochemical staining and microscopy

The mouse brain tissue was cryosectioned (14 μm thick slices) by using Thermo Scientific CryoStar NX70 (Thermo Fisher Scientific Inc, UK). Sections were kept at −80°C before use. Sections were air-dried, washed with 0.1 mol/L PBS and blocking solution containing 10% normal donkey serum (Jackson ImmunoResearch Europe Ltd, Cambridgeshire, UK), 2% bovine serum albumin and 0.3% Triton X-100 for 1 hour at room temperature (RT, 20-22°C). Slides were later incubated with the primary antibody, rabbit anti-insulin receptor antibody (1:300, insulin 1β C-19 Santa Cruz sc-711, Heidelberg, Germany) overnight at 4°C, followed by incubation with the secondary antibody, Biotin-SP (long spacer) affinipure donkey anti-rabbit IgG (H + L) antibody (1:1200 Jackson ImmunoResearch Europe Ltd, Cambridgeshire, UK). Slides were incubated in avidin/biotinylated enzyme complex solution at (RT, 30 minutes), and then developed in 3,3'-diaminobenzidine solution (RT, 5 minutes) (Vectastain® ABCsystem, Vector Laboratories, Burlingame, USA). After washing, mounting medium and coverslips were added, slides were air-dried (RT, 1 hour) and sealed with nail polish. Images were obtained using a bright-field microscope (Axioplan2 imaging, Zeiss, Germany or Olympus BX53 light microscope, Olympus corporation, Japan).

5.5.4 | Detection of neuritic plaques

Neuritic plaques were detected by Thioflavin S stain[98] with modifications. Briefly, the slices (350 μm) after electrophysiological recordings were fixed in 4% FA overnight. After that the slices were subsequently washed in phosphate buffer solution (6 times × 10 minutes), 70% ethanol (10 minutes), 80% ethanol (10 minutes). Then, the slices were incubated in 0.1% Thioflavin S solution for 2 hour on shaker protected from light. Following subsequent washes in 80% and 70% ethanol (for 10 minutes in each) and with distilled water (twice × 10 minutes), the sections were mounted in tissue mounting medium (Sigma-Aldrich, Germany). The green fluorescence stained plaques were visualized and imaged with LSM 700 laser scanning microscope (Carl Zeiss Microscopy GmbH, Germany).

5.6 | Hippocampal slice electrophysiological experiments

5.6.1 | Hippocampal slice preparation

Brain slices from the dorsal and ventral mouse hippocampus were prepared as described previously.[29,99] Briefly, following cervical dislocation, the brain was quickly removed from the skull and immersed into ice-cold N-methyl D-glucamine (NMDG)-based dissection solution (in mmol/L): 93 NMDG, 2.5 KCl, 1.2 NaH_2PO_4, 30 $NaHCO_3$, 20 HEPES, 10 $MgSO_4$, 0.5 $CaCl_2$, 5 sodium ascorbate, 2 thiourea, 3 sodium pyruvate, 12 N-acetyl-L-cysteine (only for 5-12 months old brain tissue), 25 D-glucose, pH 7.3-7.4 adjusted with 37% hydrochloric acid when oxygenated with 95% O_2 and 5% CO_2; osmolarity 300-305 mOsm adjusted with sucrose. The 350 μm thick dorsal (coronal sections) and ventral (horizontal sections) hippocampal slices were sectioned with a vibrating blade microtome Leica VT1200 S (Leica Microsystems AB, City, Germany). Freshly cut slices were transferred to a NMDG-based solution at 32°C for 12-15 minutes (8-10 weeks old mice) or 10 minutes (5-12 months old mice) and then, transferred to a chamber containing a HEPES-holding solution (in mmol/L): 92 NaCl, 2.5 KCl, 1.2 NaH_2PO_4, 30 $NaHCO_3$, 20 HEPES, 2 $MgSO_4$, 2 $CaCl_2$, 5 sodium ascorbate, 2 thiourea, 3 sodium pyruvate, 25 D-glucose, pH 7.3 - 7.4 adjusted with NaOH when bubbled with 95% O_2 and 5% CO_2, RT and osmolarity 300 - 305 mOsm adjusted with sucrose. HEPES-holding solution for slices from 5 to 12 months old mice contained 12 mmol/L N-acetyl-L-cysteine[99] osmolarity 305-308 mOsm. Slices were incubated for at least 1 hour prior to recording.

5.6.2 | Electrophysiology

GABA-activated currents were recorded from DG granule cells and CA3 pyramidal neurons in dorsal and ventral hippocampal slices using whole-cell patch-clamp electrophysiology as previously described.[29,100] Briefly, each slice was placed into a recording chamber and continuously perfused (1.5-2 mL/min) with oxygenated artificial cerebrospinal fluid (ACSF) that contained (in mmol/L): 119 NaCl, 2.5 KCl, 1.3 $MgSO_4$, 1 NaH_2PO_4, 26.2 $NaHCO_3$, 2.5 $CaCl_2$ and 11 D-glucose, pH 7.3-7.4; osmolarity 300-303 mOsm adjusted with sucrose. In order to isolate GABA-activated currents from the excitatory neurotransmission all recordings were performed in the constant presence of 3 mmol/L kynurenic acid which blocks glutamate-activated ion channels. The borosilicate glass patch pipettes had 3.4-4.1 MΩ resistance when filled with the internal solution (in mmol/L): 140 CsCl, 8 NaCl, 2 EGTA, 0.2 $MgCl_2$, 10 HEPES, 2 MgATP, 0.3 Na_3GTP, 5 QX314Br, pH 7.2 adjusted with CsOH, osmolarity 285-290 mOsm. Voltage-clamp recordings were made at RT at the holding potential of −60 mV, filtered at 2 kHz using Axoclamp 200B amplifier/Multipatch 700B amplifier (Axon Instruments, Molecular Devices, CA, USA), Axon Digidata board 1440A/1550A (Molecular Devices, CA, USA) and controlled by pCLAMP 10.5 software (Axon Instruments, Molecular Devices, CA, USA).

5.6.3 | Experimental design

sIPSCs were recorded for at least 5 minutes after baseline stabilization. To record mIPSCs, tetrodotoxin (TTX, 1 μmol/L, bath application for 10-12 minutes) was added to the ACSF to block voltage-activated sodium channels and, therefore, action potential-dependent GABA release.[27] To reveal the extrasynaptic $GABA_A$ receptors mediated currents, 100 μmol/L picrotoxin, bicuculline methiodide or SR95531 was applied.

Insulin (1 nmol/L) was either acutely applied, to the slices for at least 10 minutes or the slices were preincubated, with insulin (1 nmol/L, RT) for at least 30 minutes, with similar results. For pharmacological examination of the intracellular signalling pathways activated by insulin; the PI3K/Akt pathway or the MAPKK/ERK pathway, the slices were exposed for at least 30 minutes to a cell membrane permeable inhibitor of either PI3K or MAPKK prior to the insulin administration. We used the wortmannin (100 nmol/L), an inhibitor of PI3K, and U0126 (2 μmol/L) or PD98059 (20 μmol/L), inhibitors of MAPKK. For the functional identification of currents mediated by $GABA_A$ receptors containing the α5-$GABA_A$ subunit, the α5-$GABA_A$ receptors antagonists L-655,708 (20-100 nmol/L) or TB21007 (100 nmol/L) were used.

5.7 | Reagents

The chemicals and drugs for electrophysiology were purchased from Sigma-Aldrich, Darmstadt, Germany unless otherwise stated. Insulin, human, recombinant (yeast) (Cat. No. 11376497001, Roche Diagnostics GmbH, Mannheim, Germany), Wortmannin, U0126, PD98059, L-655,708 and TB21007 (Tocris Bioscience, Bio-Techne Ltd, Abingdon, UK). Tetrodotoxin (citrate) (TTX, Alomone labs Ltd., Jerusalem, Israel). For the stock solutions the picrotoxin, wortmannin, U0126, PD98059, L-655,708 and TB21007 were dissolved in dimethyl sulfoxide (DMSO) whereas bicuculline and TTX were dissolved directly in the ACSF. The final concentration of DMSO in the ACSF did not exceed 0.1% (v/v).

Thioflavin S was purchased from Santa Cruz Biotechnology, Inc (USA). For immunohistochemistry we used PK-6100 standart Vectastain ABC kit and DAB Peroxidase Substrate kit SK-4100 from Vector Laboratories (USA).

5.8 | Data analysis

The GABA-activated currents were studied as previously described.[29] In brief, the sIPSCs and mIPSCs were analysed using MiniAnalysis software 6.0 (Synaptosoft, Decatur, GA, USA). As the frequency of IPSCs differs between DG granule cells and CA3 pyramidal neurons, we used time (3-5 minutes) and the number of events (200-300 events), respectively, for the analysis. IPSC events were detected if larger than a threshold value, set as 5 × RMS (root-mean-square of the baseline noise), and visually inspected to remove false events. In analysis of the currents, only IPSC events with a single peak were used (10%-90% rising time ≤5 ms, current decay (ms), charge transfer Q (fC)). The total synaptic current ($sIPSC_T$ or $mIPSC_T$) was defined as frequency (s^{-1}) × Q (fC) for the individual neuron. The amplitude of the persistent extrasynaptic current was measured as the shift of the basal current baseline after application of a $GABA_A$ receptors inhibitor, picrotoxin, bicuculline or SR95531 as described previously[29,32,34,100] (pCLAMP 10.5 software, Axon Instruments, Molecular Devices, San Jose, CA, USA). As the neurons varied in size, the $IPSC_T$ and the extrasynaptic current amplitude were normalized to the cell membrane capacitance (Cm (pF)) and expressed as total synaptic current density, $sIPSC_T$ density, $mIPSC_T$ density or extrasynaptic current density (pA/pF), respectively. Only three immature granule cells were identified in dorsal DG (8-10 weeks old mice) based on electrophysiological properties and were excluded from the present study but the data obtained from these cells is presented in Figure S10.

5.9 | Statistics

The data were analysed using GraphPad Prism 8 (GraphPad Software La Jolla, CA, USA). Data were also analysed using the Wilcoxon matched-pairs signed rank test (Wilcoxon test) for parameter comparison obtained from the same cells before and after the drug application and non-parametric Mann-Whitney *U* test (MW *U* test) for comparison between two independent groups. Values are expressed as mean ± SEM (Standard Error of the mean) and n represents number of cells. A *P*-value less than .05 was statistically significant.

ACKNOWLEDGEMENTS

We thank professor Costas Papatheodoropoulos, University of Patras, Greece, for critical comments on the manuscript.

CONFLICT OF INTEREST

No potential conflict of interest relevant to this article were reported.

AUTHOR CONTRIBUTIONS

BB, ZJ, SVK proposed the study, BB, ZJ, ON, SVK, HH, JPL designed research; HH, ON did electrophysiological experiments, HH with focus on the young mice and ON with focus on the older, tg-APPSwe mice; AST, ON did the histology; ZJ, JPL suggested use of tg-APPSwe animals; ON, HH,

SVK, ZJ, AST, and BB analyzed data; ON made the figures; BB, ON and HH wrote the manuscript with input from all other authors.

DATA AVAILABILITY STATEMENT

The dataset that support the findings of this study are available from the corresponding author upon reasonable request.

ORCID

Olga Netsyk https://orcid.org/0000-0001-6869-7834
Sergiy V. Korol https://orcid.org/0000-0001-8279-2790
Zhe Jin https://orcid.org/0000-0002-4717-1558
Bryndis Birnir https://orcid.org/0000-0002-1763-0266

REFERENCES

1. Rorsman P, Braun M. Regulation of insulin secretion in human pancreatic islets. *Annu Rev Physiol*. 2013;75:155-179.
2. Kleinridders A, Ferris HA, Cai W, Kahn CR. Insulin action in brain regulates systemic metabolism and brain function. *Diabetes*. 2014;63:2232-2243.
3. Ferrario CR, Reagan LP. Insulin-mediated synaptic plasticity in the CNS: Anatomical, functional and temporal contexts. *Neuropharmacology*. 2018;136:182-191.
4. Soto M, Cai W, Konishi M, Kahn CR. Insulin signaling in the hippocampus and amygdala regulates metabolism and neurobehavior. *Proc Natl Acad Sci USA*. 2019;116:6379-6384.
5. Lathe R. Hormones and the hippocampus. *J Endocrinol*. 2001;169:205-231.
6. Havrankova J, Roth J, Brownstein M. Insulin receptors are widely distributed in the central nervous system of the rat. *Nature*. 1978;272:827-829.
7. Baura GD, Foster DM, Porte D Jr, et al. Saturable transport of insulin from plasma into the central nervous system of dogs in vivo. A mechanism for regulated insulin delivery to the brain. *J Clin Invest*. 1993;92:1824-1830.
8. Gray SM, Meijer RI, Barrett EJ. Insulin regulates brain function, but how does it get there? *Diabetes*. 2014;63:3992-3997.
9. Kuwabara T, Kagalwala MN, Onuma Y, et al. Insulin biosynthesis in neuronal progenitors derived from adult hippocampus and the olfactory bulb. *EMBO Mol Med*. 2011;3:742-754.
10. Csajbok EA, Tamas G. Cerebral cortex: a target and source of insulin? *Diabetologia*. 2016;59:1609-1615.
11. Lee JH, Jahrling JB, Denner L, Dineley KT. Targeting insulin for Alzheimer's disease: mechanisms, status and potential directions. *J Alzheimers Dis*. 2018;64:S427-S453.
12. Calvo-Ochoa E, Arias C. Cellular and metabolic alterations in the hippocampus caused by insulin signalling dysfunction and its association with cognitive impairment during aging and Alzheimer's disease: studies in animal models. *Diabetes Metab Res Rev*. 2015;31:1-13.
13. Kullmann S, Heni M, Hallschmid M, Fritsche A, Preissl H, Haring HU. Brain insulin resistance at the crossroads of metabolic and cognitive disorders in humans. *Physiol Rev*. 2016;96:1169-1209.
14. McGregor G, Malekizadeh Y, Harvey J. Minireview: Food for thought: regulation of synaptic function by metabolic hormones. *Mol Endocrinol*. 2015;29:3-13.
15. Baranowska-Bik A, Bik W. Insulin and brain aging. *Prz Menopauzalny*. 2017;16:44-46.
16. Ferreira LSS, Fernandes CS, Vieira MNN, De Felice FG. Insulin resistance in Alzheimer's disease. *Front Neurosci*. 2018;12:830.
17. Hofman A, Ott A, Breteler MM, et al. Atherosclerosis, apolipoprotein E, and prevalence of dementia and Alzheimer's disease in the Rotterdam Study. *Lancet*. 1997;349:151-154.
18. de la Monte SM. Brain insulin resistance and deficiency as therapeutic targets in Alzheimer's disease. *Curr Alzheimer Res*. 2012;9:35-66.
19. Benedict C, Kern W, Schultes B, Born J, Hallschmid M. Differential sensitivity of men and women to anorexigenic and memory-improving effects of intranasal insulin. *J Clin Endocrinol Metab*. 2008;93:1339-1344.
20. Selkoe DJ. Alzheimer's disease is a synaptic failure. *Science*. 2002;298:789-791.
21. Luchetti S, Huitinga I, Swaab DF. Neurosteroid and GABA-A receptor alterations in Alzheimer's disease. Parkinson's dIsease and multiple sclerosis. *Neuroscience*. 2011;191:6-21.
22. Rissman RA, Mobley WC. Implications for treatment: GABAA receptors in aging, Down syndrome and Alzheimer's disease. *J Neurochem*. 2011;117:613-622.
23. Limon A, Reyes-Ruiz JM, Miledi R. Loss of functional GABA(A) receptors in the Alzheimer diseased brain. *Proc Natl Acad Sci USA*. 2012;109:10071-10076.
24. Liepert J, Bar KJ, Meske U, Weiller C. Motor cortex disinhibition in Alzheimer's disease. *Clin Neurophysiol*. 2001;112:1436-1441.
25. Otis TS, Staley KJ, Mody I. Perpetual inhibitory activity in mammalian brain slices generated by spontaneous GABA release. *Brain Res*. 1991;545:142-150.
26. Soltesz I, Smetters DK, Mody I. Tonic inhibition originates from synapses close to the soma. *Neuron*. 1995;14:1273-1283.
27. Edwards FA, Konnerth A, Sakmann B. Quantal analysis of inhibitory synaptic transmission in the dentate gyrus of rat hippocampal slices: a patch-clamp study. *J Physiol*. 1990;430:213-249.
28. Otis TS, Mody I. Modulation of decay kinetics and frequency of GABAA receptor-mediated spontaneous inhibitory postsynaptic currents in hippocampal neurons. *Neuroscience*. 1992;49:13-32.
29. Netsyk O, Hammoud H, Korol SV, Jin Z, Tafreshiha AS, Birnir B. Tonic GABA-activated synaptic and extrasynaptic currents in dentate gyrus granule cells and CA3 pyramidal neurons along the mouse hippocampal dorsoventral axis. *Hippocampus*. 2020.30(11):1146–1157.
30. Birnir B, Everitt AB, Gage PW. Characteristics of GABAA channels in rat dentate gyrus. *J Membr Biol*. 1994;142:93-102.
31. Birnir B, Everitt AB, Lim MS, Gage PW. Spontaneously opening GABA(A) channels in CA1 pyramidal neurones of rat hippocampus. *J Membr Biol*. 2000;174:21-29.
32. Bai D, Zhu G, Pennefather P, Jackson MF, MacDonald JF, Orser BA. Distinct functional and pharmacological properties of tonic and quantal inhibitory postsynaptic currents mediated by gamma-aminobutyric acid(A) receptors in hippocampal neurons. *Mol Pharmacol*. 2001;59:814-824.
33. Brickley SG, Cull-Candy SG, Farrant M. Development of a tonic form of synaptic inhibition in rat cerebellar granule cells resulting from persistent activation of GABAA receptors. *J Physiol*. 1996;497(Pt 3):753-759.
34. Semyanov A, Walker MC, Kullmann DM. GABA uptake regulates cortical excitability via cell type-specific tonic inhibition. *Nat Neurosci*. 2003;6:484-490.

35. Rossi DJ, Hamann M. Spillover-mediated transmission at inhibitory synapses promoted by high affinity alpha6 subunit GABA(A) receptors and glomerular geometry. *Neuron*. 1998;20:783-795.
36. Wlodarczyk AI, Sylantyev S, Herd MB, et al. GABA-independent GABAA receptor openings maintain tonic currents. *J Neurosci*. 2013;33:3905-3914.
37. Busche MA, Chen X, Henning HA, et al. Critical role of soluble amyloid-beta for early hippocampal hyperactivity in a mouse model of Alzheimer's disease. *Proc Natl Acad Sci USA*. 2012;109:8740-8745.
38. Busche MA, Konnerth A. Impairments of neural circuit function in Alzheimer's disease. *Philos Trans R Soc Lond B Biol Sci*. 2016;371.
39. Wu Z, Guo Z, Gearing M, Chen G. Tonic inhibition in dentate gyrus impairs long-term potentiation and memory in an Alzheimer's [corrected] disease model. *Nat Commun*. 2014;5:4159.
40. Jo S, Yarishkin O, Hwang YJ, et al. GABA from reactive astrocytes impairs memory in mouse models of Alzheimer's disease. *Nat Med*. 2014;20:886-896.
41. Pike CJ, Cummings BJ, Monzavi R, Cotman CW. Beta-amyloid-induced changes in cultured astrocytes parallel reactive astrocytosis associated with senile plaques in Alzheimer's disease. *Neuroscience*. 1994;63:517-531.
42. Gasparini L, Gouras GK, Wang R, et al. Stimulation of beta-amyloid precursor protein trafficking by insulin reduces intraneuronal beta-amyloid and requires mitogen-activated protein kinase signaling. *J Neurosci*. 2001;21:2561-2570.
43. Palovcik RA, Phillips MI, Kappy MS, Raizada MK. Insulin inhibits pyramidal neurons in hippocampal slices. *Brain Res*. 1984;309:187-191.
44. Jin Z, Jin Y, Kumar-Mendu S, Degerman E, Groop L, Birnir B. Insulin reduces neuronal excitability by turning on GABA(A) channels that generate tonic current. *PLoS One*. 2011;6:e16188.
45. Milior G, Di Castro MA, Sciarria LP, et al. Electrophysiological properties of CA1 pyramidal neurons along the longitudinal axis of the mouse hippocampus. *Sci Rep*. 2016;6:38242.
46. Schreurs A, Sabanov V, Balschun D. Distinct properties of long-term potentiation in the dentate gyrus along the dorsoventral axis: influence of age and inhibition. *Sci Rep*. 2017;7:5157.
47. Malik R, Dougherty KA, Parikh K, Byrne C, Johnston D. Mapping the electrophysiological and morphological properties of CA1 pyramidal neurons along the longitudinal hippocampal axis. *Hippocampus*. 2016;26:341-361.
48. Maggio N, Segal M. Unique regulation of long term potentiation in the rat ventral hippocampus. *Hippocampus*. 2007;17:10-25.
49. Petrides T, Georgopoulos P, Kostopoulos G, Papatheodoropoulos C. The GABAA receptor-mediated recurrent inhibition in ventral compared with dorsal CA1 hippocampal region is weaker, decays faster and lasts less. *Exp Brain Res*. 2007;177:370-383.
50. Papatheodoropoulos C. Striking differences in synaptic facilitation along the dorsoventral axis of the hippocampus. *Neuroscience*. 2015;301:454-470.
51. Bragdon AC, Taylor DM, Wilson WA. Potassium-induced epileptiform activity in area CA3 varies markedly along the septotemporal axis of the rat hippocampus. *Brain Res*. 1986;378:169-173.
52. Gilbert M, Racine RJ, Smith GK. Epileptiform burst responses in ventral vs dorsal hippocampal slices. *Brain Res*. 1985;361:389-391.
53. Papatheodoropoulos C. Electrophysiological evidence for long-axis intrinsic diversification of the hippocampus. *Front Biosci (Landmark Ed)*. 2018;23:109-145.
54. Dougherty KA, Islam T, Johnston D. Intrinsic excitability of CA1 pyramidal neurones from the rat dorsal and ventral hippocampus. *J Physiol*. 2012;590:5707-5722.
55. Strange BA, Witter MP, Lein ES, Moser EI. Functional organization of the hippocampal longitudinal axis. *Nat Rev Neurosci*. 2014;15:655-669.
56. Talbot K, Wang HY, Kazi H, et al. Demonstrated brain insulin resistance in Alzheimer's disease patients is associated with IGF-1 resistance, IRS-1 dysregulation, and cognitive decline. *J Clin Invest*. 2012;122:1316-1338.
57. Hortnagl H, Tasan RO, Wieselthaler A, Kirchmair E, Sieghart W, Sperk G. Patterns of mRNA and protein expression for 12 GABAA receptor subunits in the mouse brain. *Neuroscience*. 2013;236:345-372.
58. Boucher J, Kleinridders A, Kahn CR. Insulin receptor signaling in normal and insulin-resistant states. *Cold Spring Harb Perspect Biol*. 2014;6(1):1–23.
59. Philipson O, Hammarstrom P, Nilsson KP, et al. A highly insoluble state of Abeta similar to that of Alzheimer's disease brain is found in Arctic APP transgenic mice. *Neurobiol Aging*. 2009;30:1393-1405.
60. Lord A, Kalimo H, Eckman C, Zhang XQ, Lannfelt L, Nilsson LN. The Arctic Alzheimer mutation facilitates early intraneuronal Abeta aggregation and senile plaque formation in transgenic mice. *Neurobiol Aging*. 2006;27:67-77.
61. Akintola AA, van Heemst D. Insulin, aging, and the brain: mechanisms and implications. *Front Endocrinol (Lausanne)*. 2015;6:13.
62. Wang Z, Jackson RJ, Hong W, et al. Human brain-derived abeta oligomers bind to synapses and disrupt synaptic activity in a manner that requires APP. *J Neurosci*. 2017;37:11947-11966.
63. Risold PY, Swanson LW. Structural evidence for functional domains in the rat hippocampus. *Science*. 1996;272:1484-1486.
64. Small SA. The longitudinal axis of the hippocampal formation: its anatomy, circuitry, and role in cognitive function. *Rev Neurosci*. 2002;13:183-194.
65. Moser E, Moser MB, Andersen P. Spatial learning impairment parallels the magnitude of dorsal hippocampal lesions, but is hardly present following ventral lesions. *J Neurosci*. 1993;13:3916-3925.
66. Canteras NS, Swanson LW. Projections of the ventral subiculum to the amygdala, septum, and hypothalamus: a PHAL anterograde tract-tracing study in the rat. *J Comp Neurol*. 1992;324:180-194.
67. Preston AR, Eichenbaum H. Interplay of hippocampus and prefrontal cortex in memory. *Curr Biol*. 2013;23:R764-773.
68. Wan Q, Xiong ZG, Man HY, et al. Recruitment of functional GABA(A) receptors to postsynaptic domains by insulin. *Nature*. 1997;388:686-690.
69. Vetiska SM, Ahmadian G, Ju W, Liu L, Wymann MP, Wang YT. GABAA receptor-associated phosphoinositide 3-kinase is required for insulin-induced recruitment of postsynaptic GABAA receptors. *Neuropharmacology*. 2007;52:146-155.
70. Trujeque-Ramos S, Castillo-Rolon D, Galarraga E, et al. Insulin regulates GABAA receptor-mediated tonic currents in the prefrontal cortex. *Front Neurosci*. 2018;12:345.
71. Accardi MV, Brown PM, Miraucourt LS, Orser BA, Bowie D. alpha6-Containing GABAA receptors are the principal mediators of inhibitory synapse strengthening by insulin in cerebellar granule cells. *J Neurosci*. 2015;35:9676-9688.

72. Maynard SA, Triller A. Inhibitory receptor diffusion dynamics. *Front Mol Neurosci*. 2019;12:313.
73. Akhtar A, Sah SP. Insulin signaling pathway and related molecules: Role in neurodegeneration and Alzheimer's disease. *Neurochem Int*. 2020;135:104707.
74. Battaglia S, Renner M, Russeau M, Come E, Tyagarajan SK, Levi S. Activity-dependent inhibitory synapse scaling is determined by gephyrin phosphorylation and subsequent regulation of GABAA receptor diffusion. *eNeuro*. 2018;5(1):1–20.
75. Duarte-Abritta B, Villarreal MF, Abulafia C, et al. Cortical thickness, brain metabolic activity, and in vivo amyloid deposition in asymptomatic, middle-aged offspring of patients with late-onset Alzheimer's disease. *J Psychiatr Res*. 2018;107:11-18.
76. Palpagama TH, Sagniez M, Kim S, Waldvogel HJ, Faull RL, Kwakowsky A. GABAA receptors are well preserved in the hippocampus of aged mice. *eNeuro*. 2019;6.
77. Kwakowsky A, Calvo-Flores Guzman B, Pandya M, Turner C, Waldvogel HJ, Faull RL. GABAA receptor subunit expression changes in the human Alzheimer's disease hippocampus, subiculum, entorhinal cortex and superior temporal gyrus. *J Neurochem*. 2018;145:374-392.
78. Mizukami K, Grayson DR, Ikonomovic MD, Sheffield R, Armstrong DM. GABAA receptor beta 2 and beta 3 subunits mRNA in the hippocampal formation of aged human brain with Alzheimer-related neuropathology. *Brain Res Mol Brain Res*. 1998;56(1-2):268-272.
79. Mizukami K, Ikonomovic MD, Grayson DR, et al. Immunohistochemical study of GABA(A) receptor beta2/3 subunits in the hippocampal formation of aged brains with Alzheimer-related neuropathologic changes. *Exp Neurol*. 1997;147:333-345.
80. Mizukami K, Ikonomovic MD, Grayson DR, Sheffield R, Armstrong DM. Immunohistochemical study of GABAA receptor alpha1 subunit in the hippocampal formation of aged brains with Alzheimer-related neuropathologic changes. *Brain Res*. 1998;799:148-155.
81. Rissman RA, De Blas AL, Armstrong DM. GABA(A) receptors in aging and Alzheimer's disease. *J Neurochem*. 2007;103:1285-1292.
82. Rissman RA, Mishizen-Eberz AJ, Carter TL, et al. Biochemical analysis of GABA(A) receptor subunits alpha 1, alpha 5, beta 1, beta 2 in the hippocampus of patients with Alzheimer's disease neuropathology. *Neuroscience*. 2003;120:695-704.
83. Iwakiri M, Mizukami K, Ikonomovic MD, et al. An immunohistochemical study of GABA A receptor gamma subunits in Alzheimer's disease hippocampus: relationship to neurofibrillary tangle progression. *Neuropathology*. 2009;29:263-269.
84. Crestani F, Keist R, Fritschy JM, et al. Trace fear conditioning involves hippocampal alpha5 GABA(A) receptors. *Proc Natl Acad Sci USA*. 2002;99:8980-8985.
85. Wang DS, Zurek AA, Lecker I, et al. Memory deficits induced by inflammation are regulated by alpha5-subunit-containing GABAA receptors. *Cell Rep*. 2012;2:488-496.
86. Beaumont V, Zhong N, Fletcher R, Froemke RC, Zucker RS. Phosphorylation and local presynaptic protein synthesis in calcium- and calcineurin-dependent induction of crayfish long-term facilitation. *Neuron*. 2001;32:489-501.
87. Liou JC, Kang KH, Chang LS, Ho SY. Mechanism of beta-bungarotoxin in facilitating spontaneous transmitter release at neuromuscular synapse. *Neuropharmacology*. 2006;51:671-680.
88. Okada T, Kawano Y, Sakakibara T, Hazeki O, Ui M. Essential role of phosphatidylinositol 3-kinase in insulin-induced glucose transport and antilipolysis in rat adipocytes. Studies with a selective inhibitor wortmannin. *J Biol Chem*. 1994;269:3568-3573.
89. Freund TF, Buzsaki G. Interneurons of the hippocampus. *Hippocampus*. 1996;6:347-470.
90. Jinno S, Kosaka T. Cellular architecture of the mouse hippocampus: a quantitative aspect of chemically defined GABAergic neurons with stereology. *Neurosci Res*. 2006;56:229-245.
91. Sebastiao I, Candeias E, Santos MS, de Oliveira CR, Moreira PI, Duarte AI. Insulin as a bridge between type 2 diabetes and Alzheimer disease - how anti-diabetics could be a solution for dementia. *Front Endocrinol (Lausanne)*. 2014;5:110.
92. Spinelli M, Fusco S, Grassi C. Brain insulin resistance and hippocampal plasticity: mechanisms and biomarkers of cognitive decline. *Front Neurosci*. 2019;13:788.
93. Jellinger KA. Morphologic diagnosis of "vascular dementia" - a critical update. *J Neurol Sci*. 2008;270:1-12.
94. Arnold SE, Arvanitakis Z, Macauley-Rambach SL, et al. Brain insulin resistance in type 2 diabetes and Alzheimer disease: concepts and conundrums. *Nat Rev Neurol*. 2018;14:168-181.
95. Korol SV, Jin Z, Babateen O, Birnir B. GLP-1 and exendin-4 transiently enhance GABAA receptor-mediated synaptic and tonic currents in rat hippocampal CA3 pyramidal neurons. *Diabetes*. 2015;64:79-89.
96. Plum L, Schubert M, Bruning JC. The role of insulin receptor signaling in the brain. *Trends Endocrinol Metab*. 2005;16:59-65.
97. Truett GE, Heeger P, Mynatt RL, Truett AA, Walker JA, Warman ML. Preparation of PCR-quality mouse genomic DNA with hot sodium hydroxide and tris (HotSHOT). *Biotechniques*. 2000;29:52-54.
98. Ly PT, Cai F, Song W. Detection of neuritic plaques in Alzheimer's disease mouse model. *J Vis Exp*. 2011.26(53):2831
99. Ting JT, Daigle TL, Chen Q, Feng G. Acute brain slice methods for adult and aging animals: application of targeted patch clamp analysis and optogenetics. *Methods Mol Biol*. 2014;1183:221-242.
100. Jin Z, Jin Y, Birnir B. GABA-activated single-channel and tonic currents in rat brain slices. *J Vis Exp*. 2011.17(53):2858

SUPPORTING INFORMATION

Additional supporting information may be found online in the Supporting Information section.

How to cite this article: Hammoud H Netsyk O Tafreshiha AS, et al. Insulin differentially modulates GABA signalling in hippocampal neurons and, in an age-dependent manner, normalizes GABA-activated currents in the tg-APPSwe mouse model of Alzheimer's disease. *Acta Physiol*. 2021;00:e13623. https://doi.org/10.1111/apha.13623